Inorganic Chemistry
Article

Inorg. Chem. **2010**, *49*, 2931–2947 **2931**
DOI: 10.1021/ic902472h

Two- and Three-Dimensional Open-Framework Uranium Arsenates: Synthesis, Structure, and Characterization

V. Koteswara Rao,[†] K. Bharathi,[†] Ramanath Prabhu,[†] Manabendra Chandra,[‡,§] and Srinivasan Natarajan*[,†]

[†]*Framework Solids Laboratory, Solid State and Structural Chemistry Unit, Indian Institute of Science, Bangalore-560 012, India, and* [‡]*Department of Inorganic and Physical Chemistry, Indian Institute of Science, Bangalore-560 012, India.* [§]*Currently at Florida State University, Florida.*

Received December 13, 2009

Hydrothermal reactions between uranium salts and arsenic pentoxide in the presence of two different amines yielded six new uranium arsenate phases exhibiting open-framework structures, ethylenediamine (*en*): $[C_2N_2H_9][(UO_2)(AsO_4)]$, **I**; $[C_2N_2H_{10}][(UO_2)F(HAsO_4)]_2\cdot 4H_2O$, **II**; $[C_2N_2H_9][U_2F_5(HAsO_4)_2]$, **III**; $[C_2N_2H_9][UF_2(AsO_4)]$, **IV**; diethylenetriamine (DETA), $[C_4N_3H_{16}][U_2F_3(AsO_4)_2(HAsO_4)]$, **V**; and $[C_4N_3H_{16}][U_2F_6(AsO_4)(HAsO_4)]$, **VI**. The structures were determined using single crystal studies, which revealed two- (**I**, **II**, **V**) and three-dimensional (**III**, **IV**, **VI**) structures for the uranium arsenates. The uranium atom, in these compounds, exhibits considerable variations in the coordination (6 to 9) that appears to have some correlation with the synthetic conditions. The water molecules in $[C_2N_2H_{10}][(UO_2)F(HAsO_4)]_2\cdot 4H_2O$, **II**, could be reversibly removed, and the dehydrated phase, $[C_2N_2H_{10}][(UO_2)F(HAsO_4)]_2$, **IIa**, was also characterized using single crystal studies. The observation of many mineralogical structures in the present compounds suggests that the hydrothermal method could successfully replicate the geothermal conditions. As part of this study, we have observed *autunite*, $Ca[(UO_2)(PO_4)]_2(H_2O)_{11}$, *metavauxite*, $[Fe(H_2O)_6][Al(OH)(H_2O)(PO_4)]_2$, *linarite*, $PbCu(SO_4)(OH)_2$, and *tancoite*, $LiNa_2H[Al(PO_4)_2(OH)]$, structures. The repeated observation of the secondary building unit, SBU-4, in many of the uranium arsenate structures suggests that these are viable building units. Optical studies on the uranium arsenate compound, $[C_4N_3H_{16}][U_2F_6(AsO_4)(HAsO_4)]$, **VI**, containing uranium in the +4 oxidation state indicates a blue emission through an upconversion process. The compound also exhibits antiferromagnetic behavior.

Introduction

The discovery of open structures in the family of aluminum phosphates[1] resulted in intense research activity in the area of framework compounds. The availability of large open spaces possessing channels and cavities along with the many possible applications in the areas of sorption, separation, and catalysis is a major impetus for the continued interest.[2] The past two decades have witnessed the emergence of a large number of compounds with a dazzling array of structures that incorporate almost all the elements of the periodic table.[3]

Open-framework structures based on arsenates have been studied over the years for their larger size ($As^{5+} = 0.335$ Å) compared to the more traditional phosphates ($P^{5+} = 0.17$ Å), which could lead to new compounds with novel structural features.[3b] Though the large size could be attractive for stabilizing newer frameworks, the inherent toxicity associated with arsenic has been an impediment in the study of arsenate structures. Arsenic acid (H_3AsO_4) is also weaker compared to phosphoric acid (H_3PO_4) and could affect the possible reactivity under hydrothermal conditions. In spite of these constraints, there have been reports of arsenate framework structures templated by organic amine molecules.[4,5] Thus, organically templated transition[4] and main group element[5] arsenates have been synthesized and characterized. Studies on the formation of lanthanide and actinide arsenates, however, are not many.[6]

*To whom correspondence should be addressed. E-mail address: snatarajan@sscu.iisc.ernet.in.

(1) Wilson, S. T.; Lok, B. M.; Messina, C. A.; Cannan, T. R.; Flanigen, E. M. *J. Am. Chem. Soc.* **1982**, *104*, 1146.

(2) (a) Maspoch, D.; Molina, D. R.; Veciana, J. *Chem. Soc. Rev.* **2007**, *36*, 770. (b) Ferey, G. *Chem. Soc. Rev.* **2008**, *37*, 191.

(3) (a) Cheetham, A. K.; Ferey, G.; Loiseau, T. *Angew. Chem., Int. Ed.* **1999**, *38*, 3268. (b) Mandal, S.; Natarajan, S. *Angew. Chem., Int. Ed.* **2008**, *47*, 4798.

(4) (a) Ekambaram, S.; Sevov, S. C. *Inorg. Chem.* **2000**, *39*, 2405. (b) Chakrabarti, S.; Natarajan, S. *Angew. Chem., Int. Ed.* **2002**, *41*, 1224. (c) Chakrabarti, S.; Pati, S. K.; Green, M. A.; Natarajan, S. *Eur. J. Inorg. Chem.* **2003**, 4395. (d) Chakrabarti, S.; Pati, S. K.; Green, M. A.; Natarajan, S. *Eur. J. Inorg. Chem.* **2004**, 3846. (e) Rao, V. K.; Natarajan, S. *Mater. Res. Bull.* **2006**, *41*, 973. (f) Rao, V. K.; Green, M. A.; Pati, S. K.; Natarajan, S. *J. Phys. Chem. B* **2007**, *111*, 12700.

(5) (a) Bu, X.; Gier, T. E.; Ferey, G. *Chem. Commun.* **1997**, 2271. (b) Chakrabarti, S.; Natarajan, S. *Dalton Trans.* **2002**, 4156. (c) Chakrabarti, S.; Natarajan, S. *Dalton Trans.* **2002**, 3874. (d) Rao, V. K.; Chakrabarti, S.; Natarajan, S. *Inorg. Chem.* **2007**, *46*, 10781.

(6) (a) Locock, A. J.; Burns, P. C. *J. Solid State Chem.* **2004**, *177*, 2675. (b) Alekseev, E. V.; Krivovichev, S. V.; Depmeier, W. *Radiochem.* **2008**, *50*, 445.

Published on Web 02/12/2010

Table 1. Summary of the Synthesis Conditions Employed for the Preparation of the Uranium Arsenates, **I**−**VI**[a]

s. no	composition	temp (°C)	time (h)	pH (initial, final)	product	dimensionality of the structure
1	1.0 $UO_2(OAc)_2\cdot 2H_2O$ + 4.0 As_2O_5 + 1.0 *en* + 250.0 H_2O	180, 200	24, 24	2.0, 2.0	$[C_2N_2H_9][(UO_2)(AsO_4)]$, **I**	2D
2	1.0 $UO_2(OAc)_2\cdot 2H_2O$ + 4.0 As_2O_5 + 2.0 *en* + 4.0 HF + 250.0 H_2O	180, 200	24, 24	3.1, 3.1	$[C_2N_2H_{10}][(UO_2)F(HAsO_4)]_2\cdot 4H_2O$, **II**	2D
3	1.0 $UO_2(OAc)_2\cdot 2H_2O$ + 4.0 As_2O_5 + 4.0 *en* + 4.0 HF + 250.0 H_2O	180, 200	24, 24	4.0, 4.0	$[C_2N_2H_9][U_2F_5(HAsO_4)_2]$, **III**	3D
4	1.0 $UO_2(OAc)_2\cdot 2H_2O$ + 4.0 As_2O_5 + 6.0 *en* + 4.0 HF + 250.0 H_2O	180, 200	24, 24	5.0, 5.0	$[C_2N_2H_9][UF_2(AsO_4)]$, **IV**	3D
5	1.0 $UO_2(OAc)_2\cdot 2H_2O$ + 4.0 As_2O_5 + 4.0 DETA + 2.0 HF + 250.0 H_2O	180, 200	24, 24	5.2, 5.2	$[C_4N_3H_{16}][U_2F_3(AsO_4)_2(HAsO_4)]$, **V**	2D
6	1.0 $UO_2(OAc)_2\cdot 2H_2O$ + 4.0 As_2O_5 + 4.0 *DETA* + 4.0 HF + 250.0 H_2O	180, 200	24, 24	5.0, 5.0	$[C_4N_3H_{16}][U_2F_6(AsO_4)(HAsO_4)]$, **VI**	3D

[a] Where *en* = ethylenediamine, DETA = diethylenetriamine.

There has been some interest in the study of uranium-based compounds in recent years. Amine templated uranium-based compounds are studied for their varied coordinations, relevance to geochemistry, and also for their possible applications in the areas of ion exchange, photocatalysis, etc.[7−13] The synthesis of phosphate and phosphite structures of uranium as well as novel fluorides of uranium have been accomplished.[7,8,13] No profound efforts, however, were made to investigate the formation of the uranium arsenate structures. As a matter of fact, one would expect a facile formation of uranium arsenates as the larger size of the arsenate would be accommodated and compensated equally by the larger uranium species. We wanted to test this hypothesis by investigating the formation of uranium arsenate frameworks using organic amines as structure-directing agents. During the course of this study, we also wanted to investigate the reactivity, the coordination preferences, and the possible relevance to the mineralogical structures in a family of uranium arsenates.

Our investigations were successful, and we have isolated six new uranium arsenates with two- and three-dimensional structures. Thus, $[C_2N_2H_9][(UO_2)(AsO_4)]$, **I**; $[C_2N_2H_{10}][(UO_2)F(HAsO_4)]_2\cdot 4H_2O$, **II**; $[C_2N_2H_{10}][(UO_2)F(HAsO_4)]_2$, **IIa**; $[C_2N_2H_9][U_2F_5(HAsO_4)_2]$, **III**; $[C_2N_2H_9][UF_2(AsO_4)]$, **IV**; $[C_4N_3H_{16}][U_2F_3(AsO_4)_2(HAsO_4)]$, **V**; and $[C_4N_3H_{16}][U_2F_6(AsO_4)(HAsO_4)]$, **VI**, have been prepared and their structures determined by single crystal X-ray diffraction studies. Of the six compounds, only **II**, **IIa**, and **VI** were found to be single phasic in nature and were examined by a variety of techniques. In this paper, we present the syntheses, structural, and related studies of the uranium arsenate compounds.

Experimental Section

Synthesis and Initial Characterization. All the compounds isolated in the present study were synthesized employing hydrothermal methods in the presence of organic amines. The compositions and conditions employed for the syntheses are provided in Table 1. In a typical synthesis for **I**, 1.011 g of As_2O_5 was added to 4.9 mL of water. To this, 0.467 g of $UO_2(CH_3COO)_2\cdot 2H_2O$ and 0.075 mL of *en* were added under continuous stirring, and the mixture was homogenized for 30 min at room temperature. The final reaction mixture with the composition 1 $UO_2(OAc)_2\cdot 2H_2O$/4 As_2O_5/1 *en*/250 H_2O was taken in a 23 mL Teflon-lined acid-digestion stainless-steel autoclave and heated at 180 °C for 24 h followed by heating at 200 °C for 24 h. The initial pH of the reaction mixture was acidic (∼2.0), and there was no appreciable change in the pH after the reaction. The products containing yellow colored crystals of different shapes and sizes were filtered, washed with distilled water, and dried at ambient conditions. For the preparation of compounds **II**−**VI**, in addition to the above mixture of compounds, we also added HF (48%) in the reaction mixture. The presence of F^- ions in the mixture resulted in the incorporation of fluoride ions as part of the framework. The use of HF in the synthesis of open-framework compounds has been well documented.[14] Though the exact role of the fluoride ions during the hydrothermal reaction is not yet clear, it has been observed that the presence of F^- ions facilitates the crystallization of the products with open structures. The incorporation of the fluoride ion as part of the framework was noticeable especially during the preparation of open structures involving Ga,[15] In,[16] and U.[7c,d,8b] The reaction conditions for the synthesis of the compounds **II**−**VI** are also summarized in Table 1. The present synthesis efforts yielded only two compounds, **II** and **VI**, as pure single phasic materials as shown by powder XRD. The observed

(7) (a) Francis, R. J.; Drewitt, M. J.; Halasyamani, P. S.; Ranganathachar, C.; O'Hare, D.; Clegg, W.; Teat, S. J. *Chem. Commun.* **1998**, 279. (b) Danis, J. A.; Runde, W. H.; Scott, B.; Fettinger, J.; Eichhorn, B. *Chem. Commun.* **2001**, 2378. (c) Doran, M. B.; Stuart, C. L.; Norquist, A. J.; O'Hare, D. *Chem. Mater.* **2004**, *16*, 565. (d) Ok, K. M.; Doran, M. B.; O'Hare, D. *Dalton Trans.* **2007**, 3325.
(8) (a) Doran, M.; Walker, S. M.; O'Hare, D. *Chem. Commun.* **2001**, 1988. (b) Mandal, S.; Chandra, M.; Natarajan, S. *Inorg. Chem.* **2007**, *46*, 7935.
(9) (a) Norquist, A. J.; Thomas, P. M.; Doran, M. B.; O'Hare, D. *Chem. Mater.* **2002**, *14*, 5179. (b) Doran, M. B.; Norquist, A. J.; O'Hare, D. *Inorg. Chem.* **2003**, *42*, 6989. (c) Doran, M. B.; Cockbain, B. E.; Norquist, A. J.; O'Hare, D. *Dalton Trans.* **2004**, 3810. (d) Doran, M. B.; Cockbain, B. E.; O'Hare, D. *Dalton Trans.* **2005**, 1774.
(10) (a) Blatov, V. A.; Serezhkina, L. B.; Serezhkin, V. N.; Trunov, V. K. *Zh. Neorg. Khim.* **1989**, *34*, 162. (b) Krivovichev, S. V.; Kahlenberg, V.; Tananaev, I. G.; Myasoedov, B. F. *Z. Anorg. Allg. Chem.* **2005**, *631*, 2358.
(11) (a) Almond, P. M.; Peper, S. M.; Bakker, E.; Albrecht-Schmitt, T. E. *J. Solid State Chem.* **2002**, *168*, 358. (b) Almond, P. M.; Albrecht-Schmitt, T. E. *Inorg. Chem.* **2002**, *41*, 1177. (c) Almond, P. M.; Albrecht-Schmitt, T. E. *Am. Mineral.* **2004**, *89*, 976.
(12) Wang, X.; Huang, J.; Jacobson, A. J. *J. Am. Chem. Soc.* **2002**, *124*, 15190.
(13) (a) Francis, R. J.; Halasyamani, P. S.; O'Hare, D. *Angew. Chem., Int. Ed.* **1998**, *37*, 2214. (b) Francis, R. J.; Halasyamani, P. S.; O'Hare, D. *Chem. Mater.* **1998**, *10*, 3131. (c) Francis, R. J.; Halasyamani, P. S.; Bee, J. S.; O'Hare, D. *J. Am. Chem. Soc.* **1999**, *121*, 1609. (d) Walker, S. M.; Halasyamani, P. S.; Allen, S. M.; O'Hare, D. *J. Am. Chem. Soc.* **1999**, *121*, 10513. (e) Allen, S.; Barlow, S.; Halasyamani, P. S.; Mosselmans, J. F. W.; O'Hare, D.; Walker, S. M.; Walton, R. I. *Inorg. Chem.* **2000**, *39*, 3791. (f) Almond, P. M.; Deakin, L.; Porter, M. J.; Mar, A.; Albrecht-Schmitt, T. E. *Chem. Mater.* **2000**, *12*, 3208. (g) Almond, P. M.; Talley, C. E.; Bean, A. C.; Peper, S. M.; Albrecht-Schmitt, T. E. *J. Solid State Chem.* **2000**, *154*, 635. (h) Almond, P. M.; Deakin, L.; Mar, A.; Albrecht-Schmitt, T. E. *J. Solid State Chem.* **2001**, *158*, 87. (i) Cahill, C. L.; Burns, P. C. *Inorg. Chem.* **2001**, *40*, 1347. (j) Almond, P. M.; Deakin, L.; Mar, A.; Albrecht-Schmitt, T. E. *Inorg. Chem.* **2001**, *40*, 886. (k) Wang, C. M.; Liao, C. H.; Lin, H. M.; Lii, K. H. *Inorg. Chem.* **2004**, *43*, 8239. (l) Wang, C. M.; Liao, C. H.; Kao, H. M.; Lii, K. H. *Inorg. Chem.* **2005**, *44*, 6294. (m) Ok, K. M.; O'Hare, D. *J. Solid State Chem.* **2007**, *180*, 446.
(14) Morris, R. E.; Weigel, S. J. *Chem. Soc. Rev.* **1997**, *26*, 309.

Table 2. (a) Crystal Data and Structure Refinement Parameters for $[C_2N_2H_9][(UO_2)(AsO_4)]$, **I**; $[C_2N_2H_{10}][(UO_2)F(HAsO_4)]_2\cdot 4H_2O$, **II**; $[C_2N_2H_9][U_2F_5(HAsO_4)_2]$, **III**; $[C_2N_2H_9][UF_2(AsO_4)]$, **IV**; $[C_4N_3H_{16}][U_2F_3(AsO_4)_2(HAsO_4)]$, **V**; and $[C_4N_3H_{16}][U_2F_6(AsO_4)(HAsO_4)]$, **VI**; and (b) Crystal Data and Structure Refinement Parameters for the *in Situ* Single Crystal XRD Studies on $[C_2N_2H_{10}][(UO_2)F(HAsO_4)]_2\cdot 4H_2O$, **II**; $[C_2N_2H_{10}][(UO_2)F(HAsO_4)]_2$, **IIa** (dehydrated phase); and $[C_2N_2H_{10}][(UO_2)F(HAsO_4)]_2\cdot 4H_2O$, **II** (rehydrated phase)

(a)

structure parameter	**I**	**II**	**III**	**IV**	**V**	**VI**
empirical formula	$U_{0.25}As_{0.25}O_{1.5}H_{2.25}N_{0.5}C_{0.5}$	$U_1As_1F_1O_8H_{10}N_1C_1$	$U_2As_2F_5O_8H_{11}N_2C_2$	$U_{0.5}As_{0.5}F_1O_2H_{4.5}N_1C_1$	$U_2As_3F_3O_{12}H_{17}N_3C_4$	$U_1As_1F_3O_4H_{8.5}N_{1.5}C_2$
fw	117.51	496.02	912.02	237.99	1057.03	487.54
T (K)	298	298	298	298	298	298
cryst syst	tetragonal	monoclinic	monoclinic	orthorhombic	triclinic	monoclinic
space group	$P4/n$	$P2_1/c$	$C2/c$	$Fddd$	$P\bar{1}$	$C2/m$
a (Å)	7.1360(10)	8.3586(15)	10.7672(3)	7.2852(6)	9.4256(3)	17.6377(11)
b (Å)	7.1360(10)	13.066(2)	8.7928(3)	15.6714(13)	10.3811(3)	8.0072(5)
c (Å)	8.623(3)	8.6101(16)	12.9900(3)	21.6630(18)	10.8498(4)	12.5801(8)
α (deg)	90.0000	90.0000	90.0000	90.0000	73.406(3)	90.0000
β (deg)	90.0000	104.346(3)	92.5780(10)	90.0000	64.818(3)	112.553(2)
γ (deg)	90.0000	90.0000	90.0000	90.0000	65.746(3)	90.0000
V (Å^3)	439.10(16)	911.1(3)	1228.57(6)	2473.2(4)	868.00(5)	1640.80(18)
Z	8	4	4	32	2	8
D (calcd)/g cm^{-3}	3.487	3.617	4.925	5.017	4.044	3.878
μ (mm^{-1})	22.217	21.455	31.785	31.580	24.405	23.821
λ (Mo Kα/Å)	0.71073	0.71073	0.71073	0.71073	0.71073	0.71073
θ range (deg)	2.36−27.99	2.90−28.01	2.99−25.99	5.20−28.05	3.21−29.42	1.75−30.63
total data collected	4772	7041	8895	4461	19060	11863
unique data	534	1997	1214	673	4243	2558
R indexes [$I > 2\sigma(I)$][a]	$R_1 = 0.0280$, $wR_2 = 0.0765$	$R_1 = 0.0311$, $wR_2 = 0.0772$	$R_1 = 0.0268$, $wR_2 = 0.1059$	$R_1 = 0.0222$, $wR_2 = 0.0494$	$R_1 = 0.0227$, $wR_2 = 0.0507$	$R_1 = 0.0422$, $wR_2 = 0.0993$
R indexes (all data)[a]	$R_1 = 0.0284$, $wR_2 = 0.0767$	$R_1 = 0.0340$, $wR_2 = 0.0784$	$R_1 = 0.0273$, $wR_2 = 0.1068$	$R_1 = 0.0269$, $wR_2 = 0.0518$	$R_1 = 0.0274$, $wR_2 = 0.0515$	$R_1 = 0.0503$, $wR_2 = 0.1025$

(b)

structure parameter	**II**	**IIa**	**IIb**
empirical formula	$U_1As_1F_1O_8H_{10}N_1C_1$	$U_1As_1F_1O_6H_6N_1C_1$	$U_1As_1F_1O_8H_{10}N_1C_1$
fw	496.02	460.02	496.02
T (K)	298	398	298
cryst syst	monoclinic	monoclinic	monoclinic
space group	$P2_1/c$	$P2_1/c$	$P2_1/c$
a (Å)	8.3586(15)	7.7976(19)	8.3586(15)
b (Å)	13.066(2)	12.9510(13)	13.066(2)
c (Å)	8.6101(16)	8.6123(14)	8.6101(16)
α (deg)	90.0000	90.0000	90.0000
β (deg)	104.346(3)	112.60(2)	104.346(3)
γ (deg)	90.0000	90.0000	90.0000
V (Å^3)	911.1(3)	802.9(2)	911.1(3)
Z	4	4	4
D (calcd)/gcm^{-3}	3.617	3.805	3.587
μ (mm^{-1})	21.455	24.311	21.455
λ (Mo Kα/Å)	0.71073	0.71073	0.71073
θ range (deg)	2.90−28.01	3.39−29.34	2.90−28.06
total data collected	7041	8092	9259
unique data	1997	1935	2014
R indexes [I > 2σ (I)][a]	$R_1 = 0.0311$, $wR_2 = 0.0772$	$R_1 = 0.0968$, $wR_2 = 0.2226$	$R_1 = 0.0744$, $_2 = 0.1730$
R indexes (all data)[a]	$R_1 = 0.0340$, $wR_2 = 0.0784$	$R_1 = 0.1448$, $wR_2 = 0.2494$	$R_1 = 0.1008$, $_2 = 0.1912$

[a] $R_1 = \sum ||F_o| - |F_c||/\sum |F_o|$; $wR_2 = \{\sum[w(F_o^2 - F_c^2)^2]/\sum[w(F_o^2)^2]\}^{1/2}$. $w = 1/[\sigma^2(F_0)^2 + (aP)^2 + bP]$, $P = [\max(F_o^2,0) + 2(F_c)^2]/3$, where $a = 0.0385$ and $b = 2.2546$ for **I**, $a = 0.0427$ and $b = 0.0000$ for **II**, $a = 0.1000$ and $b = 0.0000$ for **III**, $a = 0.0316$ and $b = 11.3700$ for **IV**, $a = 0.0289$ and $b = 0.0000$ for **V**, $a = 0.0556$ and $b = 0.6465$ for **VI**, $a = 0.0427$ and $b = 0.0000$ for **II**, $a = 0.1044$ and $b = 99.1428$ for **IIa**, $a = 0.1318$ and $b = 0.0000$ for **IIb**.

XRD patterns of **II** and **VI** were consistent with the XRD patterns simulated on the basis of the structure determined using the single-crystal X-ray diffraction (Figures S1 and S2, Supporting Information). The two compounds, **II** and **VI**, were characterized in detail. The powder XRD patterns of the other compounds exhibited additional diffraction peaks that did not correspond to any of the known phases including the starting

(15) (a) Chen, J.; Li, L.; Yang, G.; Xu, R. *Chem. Commun.* **1989**, 1217. (b) Luo, S. H.; Jiang, Y. C.; Wang, S. L.; Kao, H. M.; Lii, K. H. *Inorg. Chem.* **2001**, *40*, 5381. (c) Loiseau, T.; Ferey, G. *Acta Crystallogr., Sect. C* **2004**, *60*, i30. (d) Ferey, G. *J. Fluorine Chem.* **1995**, *72*, 187. (e) Loiseau, T.; Ferey, G. *J. Fluorine Chem.* **2007**, *128*, 413. (f) Choyke, S. J.; Blau, S. M.; Larner, A. A.; Sarjeant, A. N.; Yeon, J.; Halasyamani, P. S.; Norquist, A. J. *Inorg. Chem.* **2009**, DOI: 10.1021/ic901770e. (g) Wang, L.; Song, T.; Fan, Y.; Wang, Y.; Xu, J.; Shi, S.; Zhu, T. *J. Solid State Chem.* **2006**, *179*, 824. (h) Wang, L.; Song, T.; Fan, Y.; Tian, Z.; Wang, Y.; Shi, S.; Xu, J. *J. Solid State Chem.* **2006**, *179*, 3400.

(16) (a) Thirumurugan, A.; Natarajan, S. *Dalton Trans.* **2003**, 3387. (b) Yi, Z.; Yang, Y.; Huang, K.; Li, G.; Chen, C.; Wang, W.; Liu, Y.; Pang, W. *J. Solid State Chem.* **2004**, *177*, 4073. (c) Chen, C.; Yi, Z.; Bi, M.; Liu, Y.; Wang, C.; Liu, L.; Zhao, Z.; Pang, W. *J. Solid State Chem.* **2006**, *179*, 1478. (d) Chen, C.; Liu, Y.; Fang, Q.; Liu, L.; Eubank, J. F.; Zhang, N.; Gong, S.; Pang, W. *Microporous Mesoporous Mater.* **2006**, *97*, 132. (e) Chen, C.; Wang, S.; Zhang, N.; Yan, Z.; Pang, W. *Microporous Mesoporous Mater.* **2007**, *106*, 1.

Table 3. Selected Bond Distances for the Compounds $[C_2N_2H_9][(UO_2)(AsO_4)]$, **I**; $[C_2N_2H_{10}][(UO_2)F(HAsO_4)]_2 \cdot 4H_2O$, **II**; $[C_2N_2H_{10}][(UO_2)F(HAsO_4)]_2$, **IIa**; $[C_2N_2H_9][U_2F_5(HAsO_4)_2]$, **III**; $[C_2N_2H_9][UF_2(AsO_4)]$, **IV**; $[C_4N_3H_{16}][U_2F_3(AsO_4)_2(HAsO_4)]$, **V**; and $[C_4N_3H_{16}][U_2F_6(AsO_4)(HAsO_4)]$, **VI**[a,b]

bond	distance, Å [BVS][21]	bond	distance, Å [BVS][21]
	I		
U(1)−O(2)	1.773(10) [1.708]	As(1)−O(3)#4	1.666(6) [1.313]
U(1)−O(1)	1.783(10) [1.675]	As(1)−O(3)	1.666(6) [1.313]
U(1)−O(3)#1	2.267(7) [0.659]	As(1)−O(3)#5	1.666(6) [1.313]
U(1)−O(3)	2.267(7) [0.659]	As(1)−O(3)#6	1.666(6) [1.313]
U(1)−O(3) #2	2.267(7) [0.659]	∑ (As−O)	5.25
U(1)−O(3)#3	2.267(7) [0.659]		
∑ (U−O)	6.01		
	II		
U(1)−O(1)	1.777(5) [1.691]	As(1)−O(3)#2	1.665(4) [1.317]
U(1)−O(2)	1.778(5) [1.688]	As(1)−O(4)	1.676(3) [1.279]
U(1)−O(3)	2.332(4) [0.569]	As(1)−O(5)#3	1.682(4) [1.258]
U(1)−F(1)#1	2.336(4) [0.565]	As(1)−O(6)	1.722(5) [1.129]
U(1)−F(1)	2.337(4) [0.564]	∑ (As−O)	4.98
U(1)−O(4)	2.371(4) [0.528]		
U(1)−O(5)	2.414(4) [0.485]		
∑ (U−O/F)	6.09		
	IIa		
U(1)−O(1)	1.781(9) [1.678]	As(1)−O(4)	1.68(2) [1.265]
U(1)−O(2)	1.792(9) [1.642]	As(1)−O(3)	1.69(2) [1.231]
U(1)−F(1)#1	2.286(17) [0.623]	As(1)−O(5)	1.70(2) [1.198]
U(1)−F(1)	2.305(18) [0.600]	As(1)−O(6)	1.73(2) [1.105]
U(1)−O(4)	2.38(2) [0.518]	∑ (As−O)	4.80
U(1)−O(5)#2	2.388(19) [0.510]		
U(1)−O(3)#3	2.40(2) [0.498]		
∑ (U−O/F)	6.07		
	IIb		
U(1)−O(1)	1.760(13) [1.748]	As(1)−O(4)	1.653(12) [1.361]
U(1)−O(2)	1.784(13) [1.668]	As(1)−O(3)#2	1.662(12) [1.328]
U(1)−F(1)	2.324(10) [0.578]	As(1)−O(5)#3	1.716(12) [1.148]
U(1)−O(3)	2.338(12) [0.562]	As(1)−O(6)	1.734(13) [1.093]
U(1)−F(1)#1	2.346(10) [0.554]	∑ (As−O)	4.93
U(1)−O(4)	2.377(11) [0.521]		
U(1)−O(5)	2.391(12) [0.507]		
∑ (U−O/F)	6.14		
	III		
U(1)−F(1)	2.254(4) [0.552]	As(1)−O(1)	1.663(5) [1.324]
U(1)−O(2)#1	2.258(5) [0.674]	As(1)−O(2)	1.671(5) [1.296]
U(1)−F(2)	2.318(4) [0.464]	As(1)−O(3)	1.679(5) [1.268]
U(1)−O(1)	2.326(5) [0.561]	As(1)−O(4)	1.708(6) [1.173]
U(1)−F(3)	2.371(4) [0.402]	∑ (As−O)	5.06
U(1)−O(3)#2	2.390(5) [0.472]		
U(1)−F(2)#3	2.462(4) [0.314]		
U(1)−O(4)#4	2.530(6) [0.323]		
U(1)−F(1)#2	2.599(5) [0.217]		
∑ (U−O/F)	3.99		
	IV		
U(1)−O(1)#1	2.227(5) [0.732]	As(1)−O(1)#4	1.666(5) [1.313]
U(1)−O(1)#2	2.227(5) [0.732]	As(1)−O(1)	1.666(5) [1.313]
U(1)−F(1)	2.273(3) [0.524]	As(1)−O(2)#4	1.679(5) [1.268]
U(1)−F(1)#3	2.273(3) [0.524]	As(1)−O(2)	1.679(5) [1.268]
U(1)−O(2)#3	2.364(4) [0.506]	∑ (As−O)	5.16
U(1)−O(2)	2.364(4) [0.506]		
U(1)−F(1)#4	2.466(4) [0.311]		
U(1)−F(1)#5	2.466(4) [0.311]		
∑ (U−O/F)	4.14		
	V		
U(1)−F(1)	2.201(3) [0.637]	U(2)−F(3)	2.247(3) [0.562]
U(1)−O(1)#1	2.229(3) [0.729]	U(2)−F(2)	2.247(3) [0.562]
U(1)−O(3)#2	2.341(3) [0.538]	U(2)−O(7)	2.273(3) [0.647]
U(1)−O(2)	2.343(4) [0.535]	U(2)−O(8)	2.292(3) [0.615]
U(1)−O(4)#1	2.356(3) [0.517]	U(2)−O(9)#3	2.361(3) [0.510]
U(1)−O(5)#1	2.416(3) [0.439]	U(2)−O(10)	2.427(3) [0.427]
U(1)−O(6)	2.430(3) [0.423]	U(2)−O(11)#3	2.472(3) [0.378]
U(1)−O(5)	2.624(3) [0.250]	U(2)−O(10)#3	2.535(3) [0.319]
∑ (U−O/F)	4.07	∑ (U−O/F)	4.02
As(1)−O(5)	1.667(3) [1.310]	As(2)−O(4)	1.662(3) [1.328]
As(1)−O(10)	1.673(3) [1.289]	As(2)−O(8)	1.666(3) [1.314]
As(1)−O(11)	1.678(3) [1.272]	As(2)−O(2)	1.680(3) [1.265]
As(1)−O(6)	1.693(3) [1.221]	As(2)−O(12)	1.730(3) [1.105]
∑ (As−O)	4.98	∑ (As−O)	5.01
As(3)−O(3)	1.679(3) [1.268]		
As(3)−O(7)	1.683(4) [1.255]		
As(3)−O(9)	1.686(3) [1.245]		
As(3)−O(1)	1.688(4) [1.238]		
∑ (As−O)	5.00		
	VI		
U(1)−O(1)	2.275(6) [0.643]	U(2)−F(3)	2.11(2) [0.814]
U(1)−O(1)#1	2.275(6) [0.643]	U(2)−F(4)	2.238(6) [0.576]
U(1)−O(2)	2.279(6) [0.636]	U(2)−F(4)#4	2.238(6) [0.576]
U(1)−O(2)#1	2.279(6) [0.636]	U(2)−O(3)	2.339(9) [0.541]
U(1)−F(1)	2.364(3) [0.410]	U(2)−F(5)	2.389(4) [0.383]
U(1)−F(1)#2	2.364(3) [0.410]	U(2)−F(5)#5	2.389(4) [0.383]
U(1)−F(2)	2.377(3) [0.395]	U(2)−O(4)	2.398(8) [0.461]
U(1)−F(2)#3	2.377(3) [0.395]	U(2)−O(5)#6	2.424(8) [0.430]
∑ (U−O/F)	4.17	∑ (U−O/F)	4.16
As(1)−O(5)	1.656(8) [1.349]	As(2)−O(3)#5	1.667(9) [1.310]
As(1)−O(2)	1.682(6) [1.258]	As(2)−O(4)	1.668(8) [1.306]
As(1)−O(2)#7	1.682(6) [1.258]	As(2)−O(1)	1.706(6) [1.179]
As(1)−O(6)	1.720(10) [1.135]	As(2)−O(1)#4	1.706(6) [1.179]
∑ (As−O)	5.00	∑ (As−O)	4.97

[a] The bond valence sum calculations are given in the brackets. [b] Symmetry transformations used to generate equivalent atoms. **I**: #1 $-x+3/2, -y+3/2, z$; #2 $-y+3/2, x, z$; #3 $y, -x+3/2, z$; #4 $-y+2, x+1/2, -z+1$; #5 $y-1/2, -x+2, -z+1$; #6 $-x+3/2, -y+5/2, z$. **II**: #1 $x, -y+1/2, z+1/2$; #2 $-x+2, -y+1, -z+1$; #3 $-x+2, y+1/2, -z+1/2$. **IIa**: #1 $x, -y+1/2, z-1/2$; #2 $-x, -y, -z+1$; #3 $x, -y+1/2, z+1/2$. **IIb**: #1 $x, -y+1/2, z+1/2$; #2 $-x+2, -y+1, -z+1$; #3 $-x+2, y+1/2, -z+1/2$. **III**: #1 $-x+3/2, -y+3/2, -z$; #2 $-x+2, -y+1, -z$; #3 $-x+2, y, -z+1/2$; #4 $x+1/2, y+1/2, z$. **IV**: #1 $-x+1/2, y-1/4, z+1/4$; #2 $x-1/4, y-1/4, -z$; #3 $-x+1/4, y, -z+1/4$; #4 $-x+3/4, -y+3/4, z$; #5 $x-1/2, -y+3/4, -z+1/4$. **V**: #1 $-x+2, -y+1, -z+1$; #2 $x-1, y, z$; #3 $-x+2, -y+2, -z+1$. **VI**: #1 $-x, y, -z+1$; #2 $-x, -y+2, -z+1$; #3 $-x, -y+1, -z+1$; #4 $x, -y+2, z$; #5 $-x, -y+2, -z+2$; #6 $-x-1/2, -y+3/2, -z+1$; #7 $x, -y+1, z$.

materials. In spite of our many repeated attempts, we have not been able to synthesize the pure phases of the compounds **I**, **III**, **IV**, and **V**.

IR spectroscopic studies (Perkin-Elmer, SPECTRUM 1000) were carried out as a KBr pellet in the range 300−4000 cm^{-1} for compounds **II** and **VI**. The spectra exhibited typical peaks corresponding to the lattice water molecule, the amine molecule, and the arsenate moiety (Figure S3, Supporting Information). The observed bands are $\nu_{(H2O)}$ = 3500−3600 cm^{-1}, $\nu_{(N-H)}$ = 3200−3400 cm^{-1}, $\nu_{(C-H)}$ = 2800−3150 cm^{-1}, $\delta_{(H2O)}$ = 1610−1630 cm^{-1}, $\delta_{(N-H)}$ = 1610−1630 cm^{-1}, $\delta_{(C-H)}$ = 1300−1500 cm^{-1}, $\nu_{(As-OH)}$ = 1100−1250 cm^{-1}, $\nu_{(N-H)}$ = 1000−1100 cm^{-1}, $\nu_{(As-O)}$ = 760−960 cm^{-1}, and $\nu_{(U-F)}$ = 360−450 cm^{-1}.

TGA studies (Mettler-Toledo TG850) of the compounds **II** and **VI** were carried out in an atmosphere of flowing oxygen (flow rate = 50 mL min^{-1}) in the temperature range 30−850 °C (heating rate = 5 °C min^{-1}; Figure S4, Supporting Information). The TGA studies on **II** indicated that the compound exhibits a two step weight loss. The initial weight loss of 7.6% in the range 80−160 °C corresponds well with the loss of the lattice water molecules (calcd 7.3%). The second continuous broad weight loss of 18% was observed in the range 260−800 °C. The final calcined product was found to be poorly crystalline by powder XRD with the majority of the XRD lines corresponding

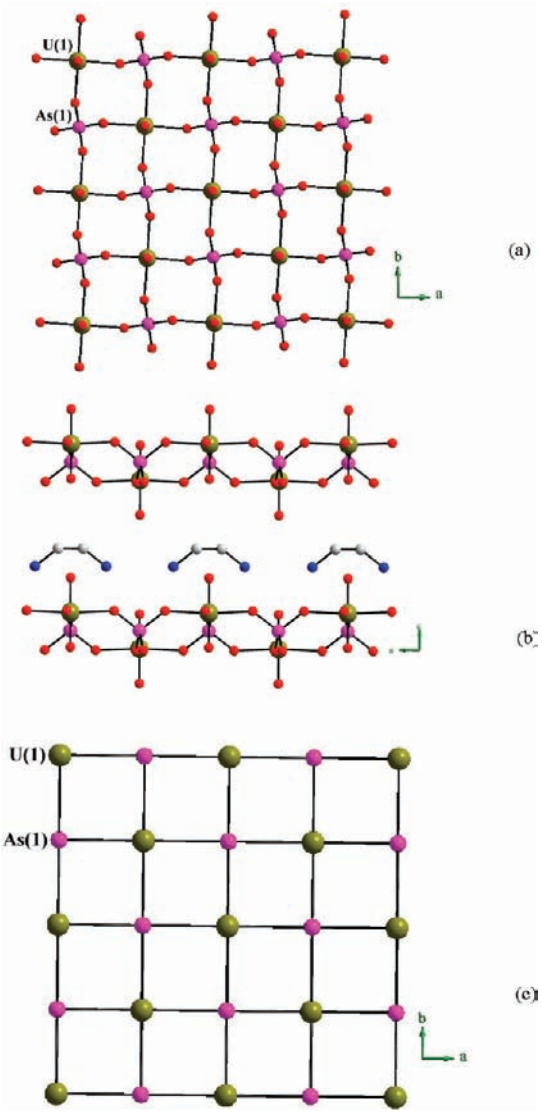

Figure 1. (a) View of a single layer in the *ab* plane in $[C_2N_2H_9][(UO_2)(AsO_4)]$, **I**. (b) View of the arrangement of the layers in the *ac* plane. Only one of the views of the disordered amine molecules is shown (see text). (c) View of the T atom [T = U (dark yellow), As (purple)] connectivity showing the (4,4) connected net structure (see text).

to the uranium arsenate phase, $UO_2(HAsO_4)$ (ICDD-10-0100). The TGA studies on **VI** indicated only one sharp weight loss of 40.9% in the range 300−350 °C. The calcined product, again, was not particularly crystalline with a majority of the observed XRD lines corresponding to the crystalline phase, UF_4 (ICDD-12-0701).

Single-Crystal Structure Determination. A suitable single crystal of each compound was carefully selected and glued to a thin glass fiber with a cyanoacrylate (superglue) adhesive. The single crystal X-ray diffraction data were collected on Bruker AXS Smart Apex CCD diffractometer at 293 K. The X-ray generator was operated at 50 kV and 35 mA using Mo Kα (λ = 0.71073 Å) radiation. Data were collected with ω scan width of 0.3°. The frames were collected in different settings of ϕ keeping the sample-to-detector distance fixed at 6.0 cm and the detector position (2θ) fixed at −25°. Pertinent experimental details of the structure determination of each compound are listed in Table 2. The data were reduced using SAINTPLUS,[17] and an empirical

(17) *SMART*, v5.628; *SAINT*, v6.45a; *XPREP*; *SHELXTL*; Bruker AXS Inc.: Madison, WI, **2004**.

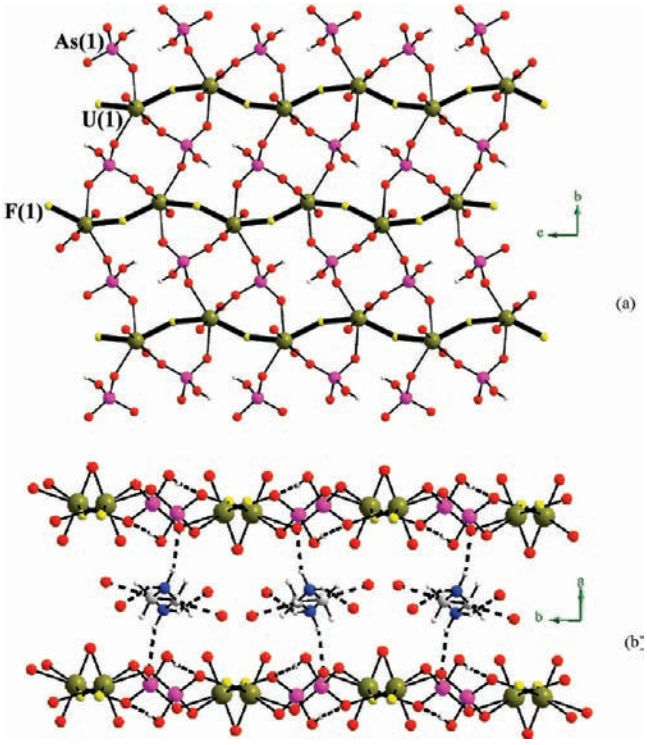

Figure 2. (a) View of a single layer in the *bc* plane in $[C_2N_2H_{10}][(UO_2)F(HAsO_4)]_2\cdot 4H_2O$, **II**. Note that the layer has 3-, 4-, and 6-membered rings. The U−F−U one-dimensional chains are highlighted (thick lines). (b) View of the arrangement of the layers in the *ab* plane. The dotted lines represent the possible hydrogen bond interactions.

absorption correction was applied using the SADABS program.[18] The crystal structures were solved and refined by direct methods using SHELXL97[19] present in the WinGx suite of programs (version 1.63.04a).[20] The amine molecules in **I**, **IV**, and **VI** were found to be disordered. The disorder of the amine molecules was modeled by keeping the bond distance considerations. The disorder of the organic amine molecules precluded anisotropic refinement for the amines in **I**, **IV**, and **VI**. Bond valence sum calculations[21] were employed to find the possible hydrogen positions for the terminal As−OH groups. The hydrogen positions for the −OH groups were placed geometrically and refined using the riding mode. The last cycles of refinements included atomic positions, anisotropic thermal parameters for all the non-hydrogen atoms, and isotropic thermal parameters for the hydrogen atoms. Full-matrix-least-squares structure refinement against $|F^2|$ was carried out using the SHELXL package of programs.[19,20] The selected bond distances are listed in Table 3. Crystallographic data (excluding structure factors) have been deposited as **I**, 380379 (CSD); **II**, 745881 (CCDC); **III**, 745882 (CCDC); **IV**, 380380 (CSD); **V**, 745883 (CCDC); and **VI**, 380378 (CSD). These data can be obtained free of charge from the Cambridge Structural Database (CSD) via http://www.fiz-karlsruhe.de/request_for_deposited_data.html and from the Cambridge Crystallographic Data Centre (CCDC) via www.ccdc.cam.ac.uk/data_request/cif.

(18) Sheldrick, G. M. *Siemens Area Detector Absorption Correction Program*; University of Göttingen: Göttingen, Germany, 1994.
(19) Sheldrick, G. M. *SHELXL-97*; University of Göttingen: Göttingen, Germany, 1997.
(20) Farrugia, J. L. *J. Appl. Crystallogr.* **1999**, *32*, 837.
(21) (a) Brown, I. D.; Altermatt, D. *Acta Crystallogr., Sect. B* **1985**, *41*, 244. (b) Brese, N. E.; O'Keeffe, M. *Acta Crystallogr., Sect. B* **1991**, *47*, 192. (c) Burns, P. C.; Ewing, R. C.; Hawthorne, F. C. *Can. Mineral.* **1997**, *35*, 1551. (d) Brown, I. D. *Chem. Rev.* **2009**, *109*, 6858.

Table 4. Important Hydrogen Bond Interactions in $[C_2N_2H_{10}][(UO_2)F(HAsO_4)]_2\cdot 4H_2O$, **II**; $[C_2N_2H_{10}][(UO_2)F(HAsO_4)]_2$, **IIa**; $[C_2N_2H_9][U_2F_5(HAsO_4)_2]$, **III**; and $[C_4N_3H_{16}][U_2F_3(AsO_4)_2(HAsO_4)]$, **V**

D−H···A	D−H (Å)	H···A (Å)	D···A (Å)	D−H···A (deg)
		II		
N(1)−H(1)···O(200)	0.89	2.00	2.810	151
N(1)−H(2)···O(4)	0.89	1.97	2.825	162
N(1)−H(3)···O(100)	0.89	2.08	2.895	152
O(200)−H(201)···O(100)	0.94	1.93	2.839	164
O(6)−H(6)···O(5)	0.82	1.90	2.710	172
		IIa		
N(1)−H(1)···O(5)	0.89	1.91	2.72	150
N(1)−H(2)···O(6)	0.89	2.09	2.84	143
N(1)−H(3)···O(2)	0.89	2.50	3.28	147
O(6)−H(6)···O(3)	0.82	1.94	2.76	175
		III		
N(1)−H(1)···O(3)	0.89	2.35	3.134	148
N(1)−H(2)···F(2)	0.89	1.81	2.625	153
N(1)−H(3)···F(1)	0.89	2.25	3.051	150
C(1)−H(5)···F(2)	0.97	2.33	3.229	153
		V		
N(1)−H(2)···O(6)	0.89	1.90	2.709	150
N(1)−H(3)···O(9)	0.89	1.98	2.865	178
N(2)−H(4)···F(3)	0.90	1.83	2.626	146
N(2)−H(5)···O(11)	0.90	2.10	2.954	157
N(3)−H(6)···O(2)	0.89	2.16	2.958	149
N(3)−H(7)···O(12)	0.89	2.00	2.872	166
N(3)−H(8)···F(1)	0.89	1.78	2.627	157
C(2)−H(11)···F(1)	0.97	2.41	3.365	166

Results

Structure of $[C_2N_2H_9][(UO_2)(AsO_4)]$, I. The asymmetric unit contains 8 non-hydrogen atoms of which one uranium and one arsenic atom are crystallographically independent. The atoms, U(1), As(1), O(1), and O(2), occupy special positions with a site multiplicity of 0.25. The uranium atom is octahedrally coordinated with six oxygen atoms (Figure S5a, Supporting Information). The U−O bond distances have an average value of 2.104 Å. We observed short U−O distances of 1.773(10) and 1.783(10) Å which correspond to the terminal U═O bonds. Both uranium and arsenic are bonded through four oxygen atoms (U−O−As) with an average bond angle of 138.6°. The As−O bond distances have an average value of 1.666 Å (Table 3). The various geometrical parameters, observed for **I**, agree well with other similar ones reported in the literature.[6,7]

The structure of **I** consists of a network of $(UO_2)O_4$ and AsO_4 polyhedral units. The strictly alternating UO_6 octahedral and AsO_4 tetrahedral units are connected through their vertices to form a layered structure (Figure 1a). The layers are stacked in an AAAA... fashion (Figure 1b). Two of the U−O linkages are terminal in **I** (U═O), which leaves four U−O−As bridges and facilitates the formation of a two-dimensional (4,4)-net structure (Figure 1c). It may be noted that the (4,4)-nets with layered structures are not common in open-framework compounds, only two such examples were known in the literature, and both of them have been observed in the family of arsenate structures.[5a,d] The disordered amine molecules occupy the interlamellar spaces (Figure 1b and Figure S5b, Supporting Information).

Structure of $[C_2N_2H_{10}][(UO_2)F(HAsO_4)]_2\cdot 4H_2O$, II. The asymmetric unit contains 13 non-hydrogen atoms of which one uranium and one arsenic atom are crystallographically independent. The uranium atom is bonded with five oxygen and two fluorine atoms forming a pentagonal bipyramidal coordination (Figure S6a, Supporting Information). The U−O and the U−F bond distances have average values of 2.134 Å and 2.336 Å. The shorter U−O bond distances of 1.777(5) Å and 1.778 Å correspond to the terminal U═O bonds. Both the uranium and arsenic are bonded through three oxygen atoms (U−O−As) with an average bond angle of 125.3°. The As(1)−O bond distances have an average value of 1.686 Å. The As−O bond, As(1)−O(6), with a bond distance of 1.722(5) Å is an As−OH linkage (Table 3).

The structure of **II** consists of a network of UO_5F_2 and $HAsO_4$ polyhedral units. The uranium atoms are connected to each other through their fluorine vertices to form a one-dimensional U−F−U chain. The chains are further connected with $HAsO_4$ units to form layers possessing 3-, 4-, and 6-membered rings in the *bc* plane (Figure 2a). The layers are stacked in an AAAA... fashion (Figure 2b). The guest molecules, the water and the amine molecules, occupy the interlamellar spaces and form O−H···O and N−H···O hydrogen bonds between themselves (Figure 2b). The water molecules, O(100) and O(200), are separated by a distance of 2.85 Å and interact with each other through the O−H···O hydrogen bond interactions (Table 4) (Figures S6b and S6c, Supporting Information). In addition, we also observed intralayer hydrogen bonding involving terminal As−OH units. The stability of the water molecules was also evaluated employing the Gaussian 98 program,[22] using the basis set of B3LYP/6-31G+G(d,p). The calculation was performed using the single point energy calculation

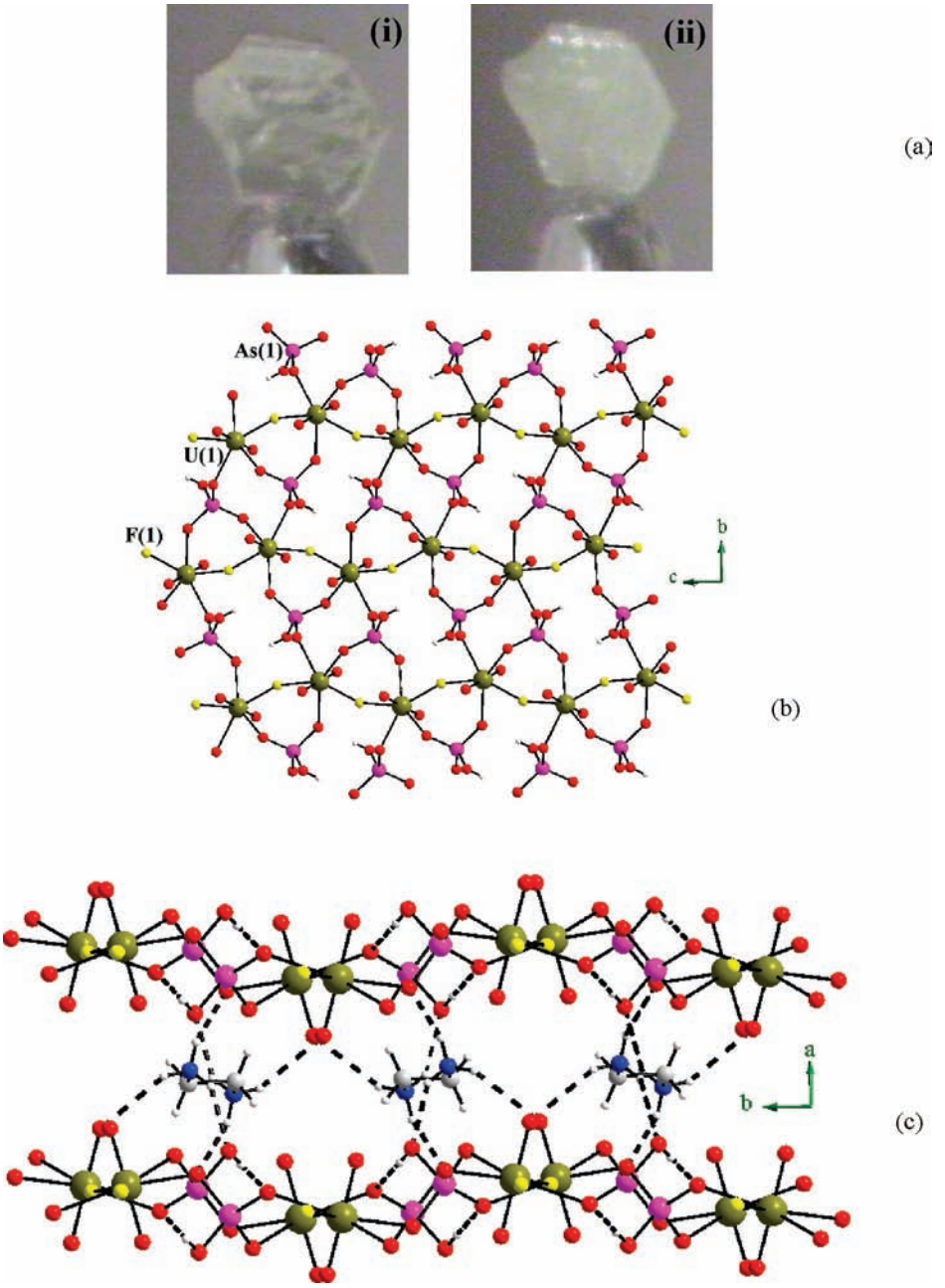

Figure 3. (a) View of the crystals: (i) 298 K, (ii) 398 K. (b) View of a single layer of the dehydrated phase in the *bc* plane $[C_2N_2H_{10}][(UO_2)F(HAsO_4)]_2$, **IIa**. Note the close similarity to **II**. (c) View of the arrangement of the layers in the *ab* plane. The dotted lines represent the possible hydrogen bond interactions. Note the absence of lattice water molecules and a slight puckering of the layers.

without any symmetry constraints. The calculated value for the stabilization was found to be −12.14 kcal/mol. This value suggests that the water molecules are reasonably stabilized in **II**. Similar values have also been observed recently.[23] The TGA studies suggested that the water molecules could be removed in the temperature range 160−250 °C (Figure S4, Supporting Information). We wanted to examine whether the guest water molecules could be removed from **II** without disturbing the layer framework structure. To this end, we have carried out single-crystal-to-single-crystal transformation studies on this phase and obtained the dehydrated phase $[C_2N_2H_{10}][(UO_2)F(HAsO_4)]_2$, **IIa**.

(22) Frisch, M. J.; Trucks, G. W.; Schlegel, H. B.; Scuseria, G. E.; Robb, M. A.; Cheeseman, J. R.; Zakrzewski, V. G.; Montgomery, J. A., Jr.; Stratmann, R. E.; Burant, J. C.; Dapprich, S.; Millam, J. M.; Daniels, A. D.; Kudin, K. N.; Strain, M. C.; Farkas, O.; Tomasi, J.; Barone, V.; Cossi, M.; Cammi, R.; Mennucci, B.; Pomelli, C.; Adamo, C.; Clifford, S.; Ochterski, J.; Petersson, G. A.; Ayala, P. Y.; Cui, Q.; Morokuma, K.; Salvador, P.; Dannenberg, J. J.; Malick, D. K.; Rabuck, A. D.; Raghavachari, K.; Foresman, J. B.; Cioslowski, J.; Ortiz, J. V.; Baboul, A. G.; Stefanov, B. B.; Liu, G.; Liashenko, A.; Piskorz, P.; Komaromi, I.; Gomperts, R.; Martin, R. L.; Fox, D. J.; Keith, T.; Al-Laham, M. A.; Peng, C. Y.; Nanayakkara, A.; Challacombe, M.; Gill, P. M. W.; Johnson, B.; Chen, W.; Wong, M. W.; Andres, J. L.; Gonzalez, C.; Head-Gordon, M.; Replogle, E. S.; Pople, J. A. *Gaussian 98*, revision A11; Gaussian, Inc.: Pittsburgh, PA, 2001.

(23) Mahata, P.; Ramya, K. V.; Natarajan, S. *Inorg. Chem.* **2009**, *48*, 4942.

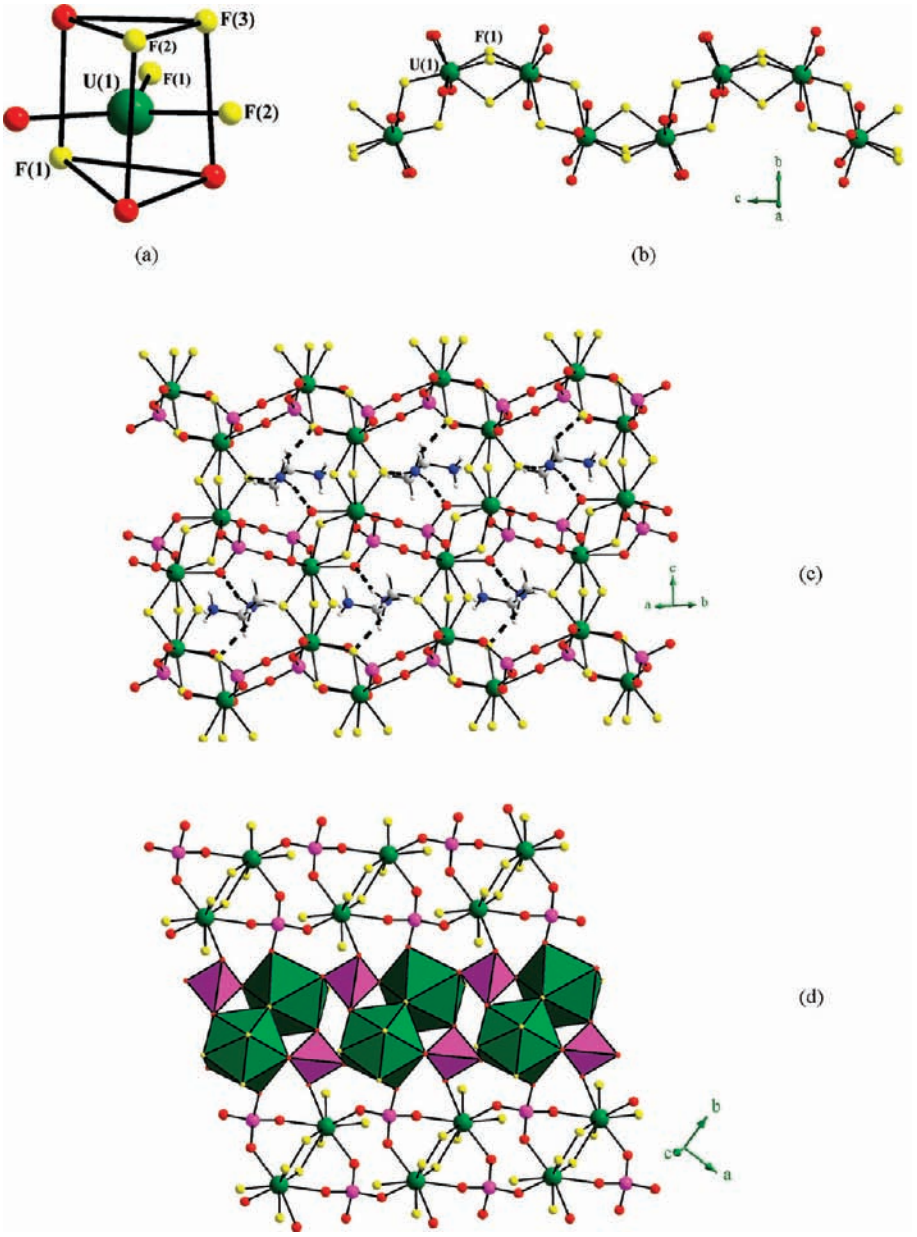

Figure 4. (a) The tricapped trigonal prismatic coordination of uranium in $[C_2N_2H_9][U_2F_5(HAsO_4)_2]$, **III**. (b) View of the one-dimensional U−F−U chain formed by the connectivity through edge- and face-shared fluorines. (c) View of the three-dimensional structure along the [110] direction. The dotted lines represent the possible hydrogen bond interactions. (d) View of the layer structure formed by the connectivity between the SBU-4 units. Note the one-dimensional chains formed from the SBU-4 units are highlighted (polyhedra).

Structure of $[C_2N_2H_{10}][(UO_2)F(HAsO_4)]_2$, IIa. The *in situ* single-crystal−single-crystal transformation studies were carried out at 125 °C (398 K). As can be noted, during the dehydration, compound **II** appears to retain the single crystalline nature (Figure 3a). The high temperature dehydrated structure could be solved, again, by the direct methods. The asymmetric unit contains 11 non-hydrogen atoms of which one uranium and one arsenic atom are crystallographically independent. Similar to **II**, the uranium atom is bonded with five oxygen and two fluorine atoms forming a pentagonal bipyramidal coordination. The various geometrical parameters associated with the dehydrated compound exhibit marginal differences compared to the hydrated phase, **II** (Table 3 and Table S1, Supporting Information).

Structurally, the removal of lattice water molecules from **II** appears to distort the layer structure slightly (Figure 3b). This distortion was, probably, necessitated as more framework oxygens participate in hydrogen bond interactions with the guest amine molecules (Figure 3c). The important hydrogen bond interactions observed in **IIa** are listed in Table 4.

Structure of $[C_2N_2H_9][U_2F_5(HAsO_4)_2]$, III. The asymmetric unit contains 10 non-hydrogen atoms of which one uranium and arsenic atom are crystallographically independent. One of the fluorine atoms, F(3), occupies a special position with a site multiplicity of 0.5. The uranium atom is bonded to four oxygen and five fluorine atoms forming a tricapped trigonal prismatic arrangement (Figure 4a). The U−O and the U−F bond distances have average values of 2.376 Å and 2.400 Å, respectively. The uranium atoms are

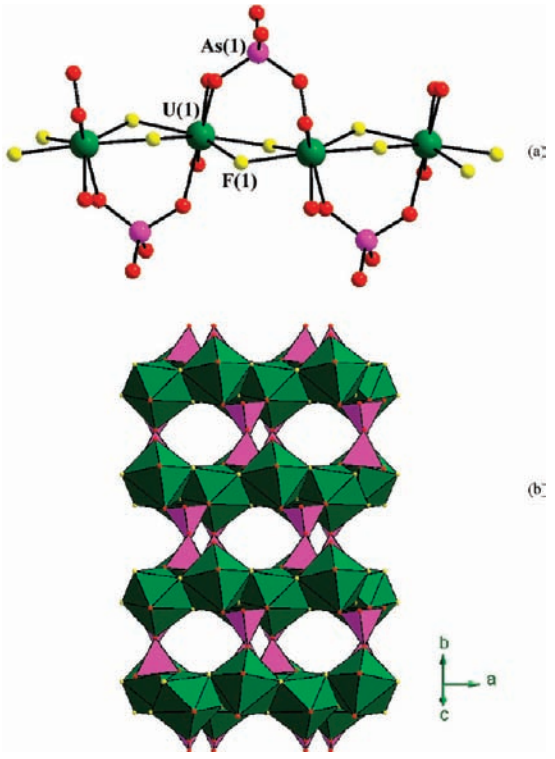

Figure 5. (a) View of the one-dimensional chain in $[C_2N_2H_9][UF_2(AsO_4)]$, **IV**. (b) The polyhedral representation of the three-dimensional structure of **IV** in the [011] direction.

bonded to arsenic atoms through four oxygen atoms (U−O−As) with an average bond angle of 139.8°. The As−O bond distances have an average value of 1.680 Å. The As−O bond, As(1)−O(4), with a bond distance of 1.708(6) Å is an As−OH linkage (Table 3).

The structure of **III** consists of a network of UO_4F_5 and $HAsO_4$ tetrahedral units. The UO_4F_5 tricapped trigonal prism units are connected to each other through their edges and faces, alternatively, via the fluorine vertices forming a one-dimensional U−F−U chain (Figure 4b). The uranium fluoride one-dimensional chains are connected through the AsO_4 units forming the three-dimensional structure (Figures 4c). The structure of **III** can also be considered to be built up from the connectivity that involves the secondary building units (SBUs).[3b] Thus, UO_4F_5 and $HAsO_4$ units are connected together forming a building unit that resembles the SBU-4 unit.[3b,15d] The SBU-4 units are connected together forming chains that are further connected through the oxygen atoms forming the two-dimensional layer structure (Figure 4d). The layers are bonded through the fluorine atoms to give rise to the three-dimensional structure. The protonated organic amine molecules, *en*, occluded in the channels participate in hydrogen bond interactions with the framework oxygen and fluorine atoms (Figure 4c). The important hydrogen bond interactions are listed in Table 4.

Structure of $[C_2N_2H_9][UF_2(AsO_4)]$, IV. The asymmetric unit contains 7 non-hydrogen atoms of which one uranium and arsenic atom are crystallographically independent, and both occupy special positions with a site multiplicity of 0.5. The uranium atom is bonded to four oxygen and four fluorine atoms forming a distorted dodecahedral arrangement (Figure S7a, Supporting Information). The U−O and U−F bond distances have average values of 2.295 Å and 2.369 Å, respectively. Both the uranium and the arsenic are bonded through four oxygen atoms (U−O−As) with average bond angle of 149.8°. The As−O bond distances have an average value of 1.672 Å (Table 3).

In **IV**, the UO_4F_4 dodecahedral units are bonded through their trans-fluorine edges forming one-dimensional U−F−U chains (Figure 5a). The AsO_4 tetrahedral units are connected to the chain and are linked together forming the three-dimensional structure with one-dimensional channels (Figure 5b and Figure S7c, Supporting Information). The disordered amine molecules occupy these channels (Figures S7b and S7c, Supporting Information).

Structure of $[C_4N_3H_{16}][U_2F_3(AsO_4)_2(HAsO_4)]$, V. The asymmetric unit contains 27 non-hydrogen atoms of which two uranium and three arsenic atoms are crystallographically independent. Of the two uranium atoms, U(1) is bonded to seven oxygens and one fluorine atom, and U(2) is bonded to six oxygens and two fluorines, forming the distorted dodecahedral coordination (Figure S8a, Supporting Information). All the fluorine atoms in **V** are terminal. The U−O and U−F bond distances have average values of 2.073 Å and 2.231 Å, respectively. All the oxygen vertices of the uranium atoms are connected to arsenic through U−O−As bonds with an average bond angle of 128.1°. Of the three arsenic atoms, As(1) and As(3) have four As−O−U bonds, while As(2) forms three such bonds and possesses one terminal As−O bond. The As−O bond distances have an average value of 1.682 Å. The As−O bond, As(2)−O(12), with a bond distance of 1.730(3) Å, is an As−OH linkage (Table 3). Similar geometrical parameters have been observed before.[6−8]

The structure of **V** consists of a network of UO_7F, UO_6F_2, AsO_4, and $HAsO_4$ polyhedral units. The two-dimensional structure of **V** can be understood by considering simpler building units. Thus, the $U(1)O_7F$ and $HAs(2)O_4$ as well as $U(2)O_6F_2$ and $As(3)O_4$ polyhedral units form two independent SBU-4 units (Figure 6a). The SBU-4 units are linked together forming a one-dimensional chain (Figure 6b). The arsenate unit, $As(1)O_4$, is bonded to this chain in such a manner that it connects to both the U(1) as well as the U(2) centers through the edges (Figures S8b and S8c, Supporting Information). It appears that the role of $As(1)O_4$ tetrahedral units is to satisfy the coordination requirement for the uranium atoms as it connects only the U(1) and the U(2) centers, which are otherwise linked through the other two arsenates, $HAs(2)O_4$ and $As(3)O_4$ (Figure S8c, Supporting Information). Edge connectivity of the tetrahedral units is not common and generally introduces great strain in the structure according to the Pauling rule.[24] The observation of such bonding in **V** is unique and noteworthy. The layer structure is formed by the connectivity between the one-dimensional chains and the $As(3)O_4$ units (Figure 6c). The layers are arranged in an ABAB... fashion, and the organic amine molecule, protonated DETA, occupies the interlamellar spaces. The amine molecule participates in extensive hydrogen bond interactions with the

(24) Burdett, J. K. *Chemical Bonding in Solids*; Oxford University Press: New York, 1995.

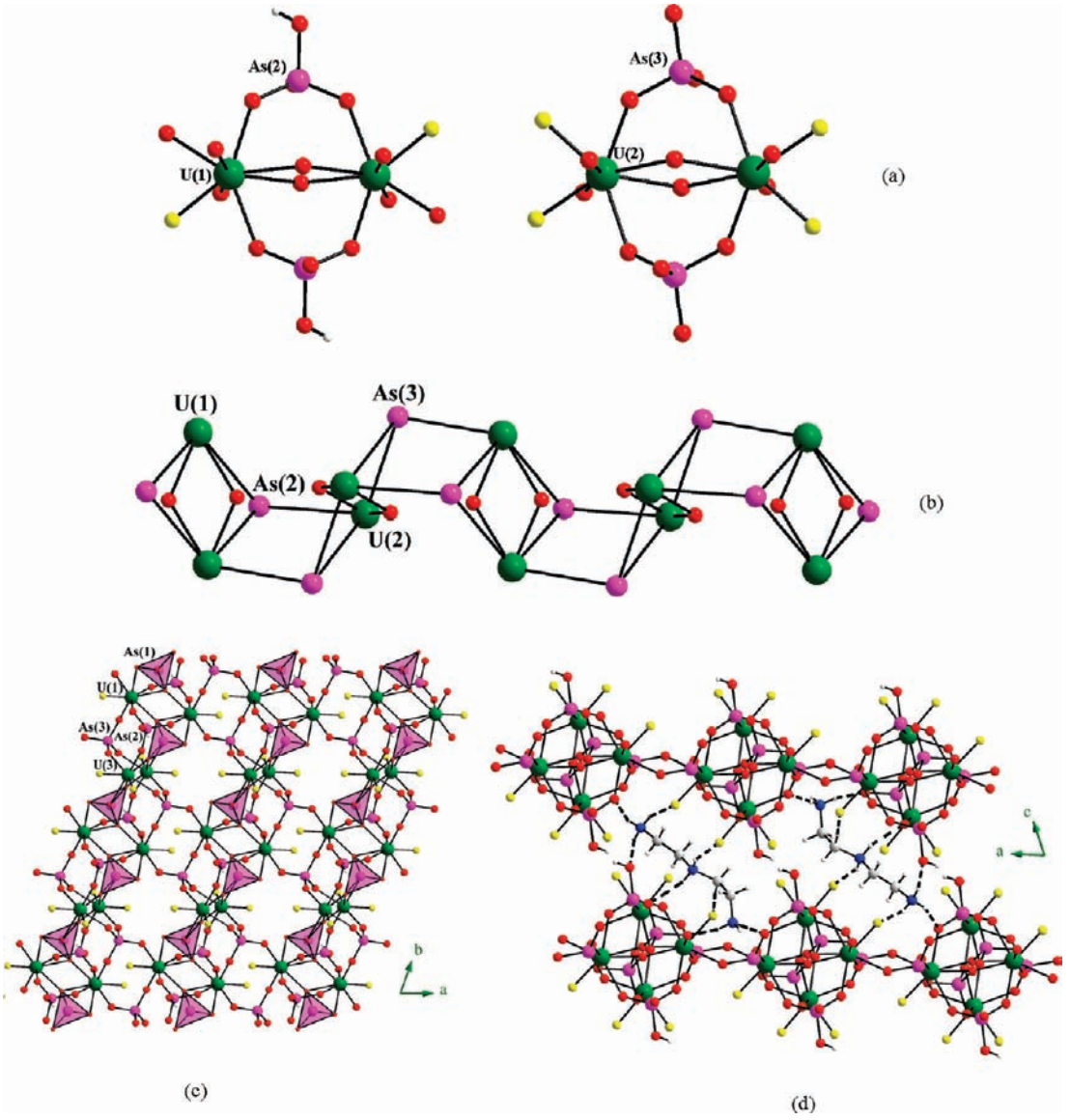

Figure 6. (a) The two different SBU-4 units observed in $[C_4N_3H_{16}][U_2F_3(AsO_4)_2(HAsO_4)]$, **V**. (b) The one-dimensional chain formed from the T-atom connectivity [T = U (olive green), As (purple)] between the two SBU-4 units. (c) View of the layer in the *ab* plane in **V**. The As(1)O_4 unit is shown as the polyhedra. Note that the As(1)O_4 unit connects only two uranium centers through the edges (see text). (d) View of the arrangement of the layers in the *ac* plane. The dotted lines represent the possible hydrogen bond interactions.

framework oxygens as well as the terminal fluorine atoms (Figure 6d). The important hydrogen bond interactions are listed in Table 4.

Structure of $[C_4N_3H_{16}][U_2F_6(AsO_4)(HAsO_4)]$, VI. The asymmetric unit contains 22 non-hydrogen atoms of which two uranium and two arsenic atoms are crystallographically independent, both of which occupy special positions with a site multiplicity of 0.5. Both the uranium atoms are 8-coordinated forming a distorted dodecahedral arrangement. U(1) is bonded to four oxygens and four fluorine atoms, and U(2) is bonded to three oxygens and five fluorine atoms (Figure S9a, Supporting Information). Many of the participating atoms, F(1), F(2), F(3), F(5), O(3), O(4), O(5), and O(6), also occupy special positions with site multiplicities of 0.5. The U−O and U−F bond distances have average values of 2.324 Å and 2.316 Å. While the U(1) atoms are connected to the arsenic through four U−O−As bonds (av. 137.7°), the U(2) atoms are connected through three U−O−As bonds (av. 142.5°). The As(1) has three As−O−U linkages, and the As(2) has four As−O−U linkages. The As−O bond distances have an average value of 1.686 Å. The As−O bond, As(1)−O(6), with a bond distance of 1.720(10) Å is an As−OH linkage (Table 3).

The structure of **VI** consists of a network of UO_4F_4, UO_3F_5, AsO_4, and $HAsO_4$ polyhedral units. The U(1)-O_4F_4 units are bonded through the trans-fluorine edges, F(1) and F(2), to form a one-dimensional chain of U−F−U. The HAs(1)O_4 and As(2)O_4 units bind with the uranium fluoride chains to form a structure that is similar to that observed in the naturally occurring mineral, *tancoite* (Figure 7a).[25c,d] The U(2)O_3F_5 units are

(25) (a) Bachmann, V. H. G.; Zemann, J. *Acta Crystallogr*. **1961**, *14*, 747. (b) Baur, W. H.; Rama Rao, B. *Natureweiss*. **1967**, *56*, 561. (c) Hawthorne, F. C. *TMPM Tschermaks Min. Petr. Mitt*. **1983**, *31*, 121. (d) Hawthorne, F. C. *Acta Crystallogr., Sect. B* **1994**, *50*, 481. (e) Locock, A. J.; Burns, P. C. *Am. Mineral*. **2003**, *88*, 240.

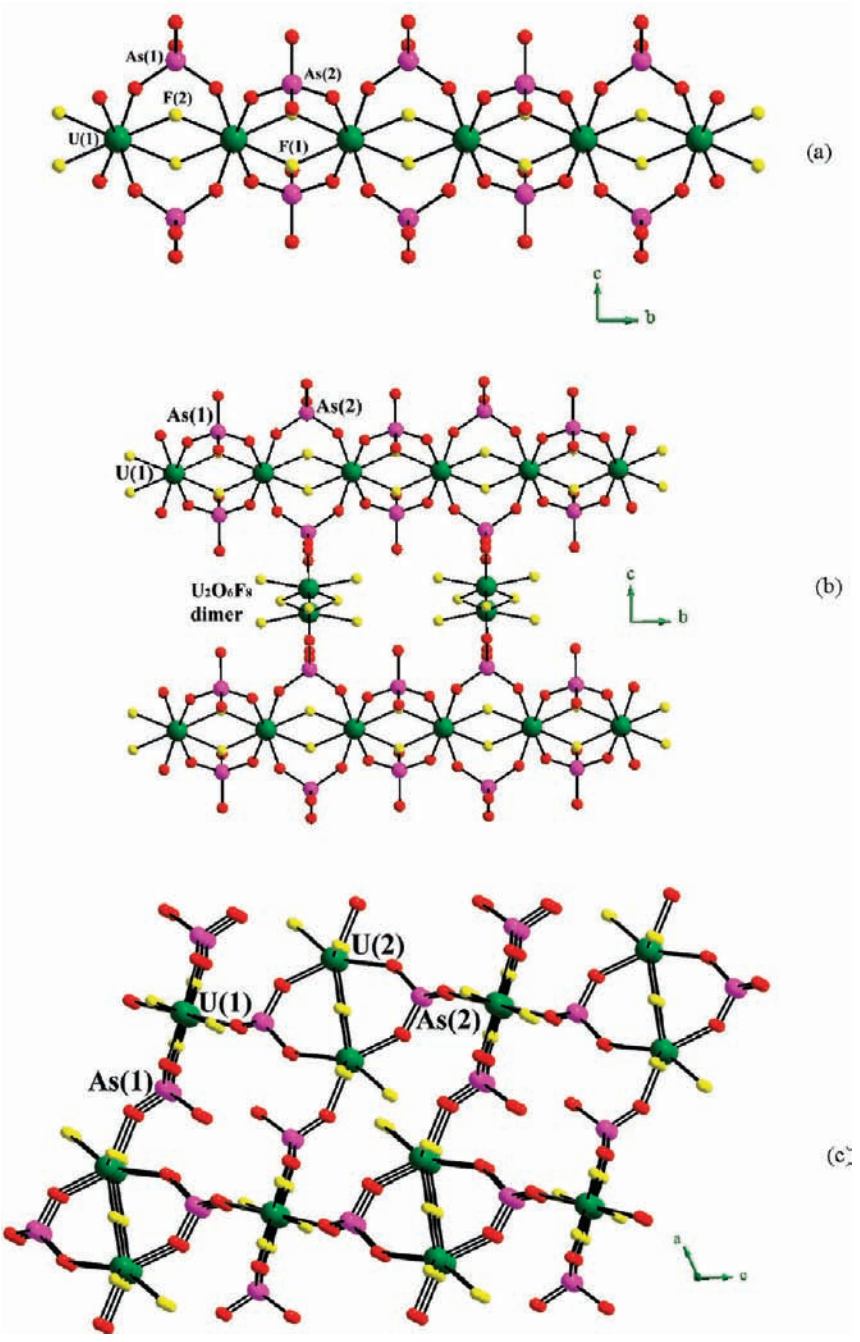

Figure 7. (a) View of the one-dimensional structure in $[C_4N_3H_{16}][U_2F_6(AsO_4)(HAsO_4)]$, **VI**. (b) View of the layer formed by the connectivity between the 1D chains and $U_2O_6F_8$ dimers through the $As(2)O_4$ tetrahedra. (c) View of the three-dimensional structure of **VI** in the *ac* plane.

connected together through the fluorine bridges, F(5), to form $U_2O_6F_8$ dimers. The fluorine atoms, F(3) and F(4), bonded to U(2) are terminal U−F linkages. The $U_2O_6F_8$ dimers link with the uranium fluoroarsenate chains, $[UF_2(AsO_4)(HAsO_4)]_\infty$, through the $As(2)O_4$ units to form a two-dimensional layer (Figures 7b). The adjacent layers are also connected through the $HAs(1)O_4$ units forming the three-dimensional structure with one-dimensional channels along the [010] direction (Figures 7c), where the disordered amine molecules occupy the channels (Figures S9c and S9d, Supporting Information). The structure of **VI** can also be described on the basis of the secondary building unit SBU-4. Thus, the $U(1)O_4F_4$, $HAs(1)O_4$, and $As(2)O_4$ units are connected to form the SBU-4 units (Figure S9b, Supporting Information). The SBU-4 units are connected through the corners forming a one-dimensional chain (Figure 7a). The chains are connected through another SBU-4 units formed by the linkages between $U(2)O_3F_5$ and $As(2)O_4$ units forming the layer (Figure 7b). The layers are further connected forming the three-dimensional structure. Thus, the structure of **VI** is the first example of a three-dimensional structure formed entirely by the connectivity between the SBU-4 units in a uranium arsenate family of compounds.

Discussion

Synthesis. Six new uranium arsenate compounds have been prepared by employing hydrothermal reactions.

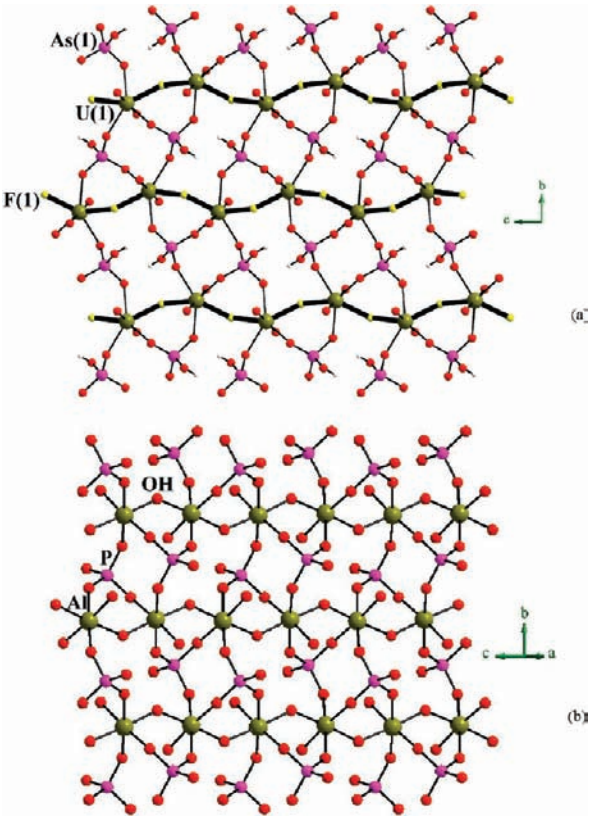

Figure 8. (a) View of a single layer in in the *bc* plane in $[C_2N_2H_{10}][(UO_2)F(HAsO_4)]_2 \cdot 4H_2O$, **II**. (b) View of a single layer in the aluminum phosphate mineral, *metavauxite*, $[Fe(H_2O)_6][Al(OH)(H_2O)(PO_4)]_2$.[25b,d]

During the course of this study, four uranium arsenate compounds (**I**−**IV**) were prepared using ethylenediamine (*en*) and two compounds (**V**−**VI**) using diethylenetriamine (DETA) in the synthesis mixture. Formation of few related phases by the use of a single amine has been known in the family of open-framework solids.[3b,4a] Presently, two 2D and 3D structures were isolated using *en* and one each of 2D and 3D structures using DETA. Typical of the hydrothermal methods, there appears to be no particular correlation between the starting reaction composition and the final solid phase product. From the composition, it appears that the increase in the quantity of *en* during the synthesis of **I**−**IV** could have helped in the deprotonation of the arsenic acid and resulted in the increase in the dimensionality of the structures (**III** and **IV**).[26] Similar observations have been made previously during the synthesis of the phosphate structures. During the use of DETA, there were no observable correlation between the composition (pH) and the dimensionality of the structures. In addition, compounds **I** and **II** have uranium in a +6 oxidation state, and in **III**−**VI**, it exists in a +4 oxidation state. Reduction of the uranium species under hydrothermal conditions has been observed before, especially in uranium phosphate and phosphite structures.[8b] It is likely that the more acidic pH of the reaction mixture in **I** and **II** would have resulted in uranium

(26) (a) Rao, C. N. R.; Natarajan, S.; Neeraj, S. *J. Am. Chem. Soc.* **2000**, *122*, 2810. (b) Choudhury, A.; Natarajan, S.; Rao, C. N. R. *Inorg. Chem.* **2000**, *39*, 4295. (c) Rao, C. N. R.; Natarajan, S.; Choudhury, A.; Neeraj, S.; Ayi, A. A. *Acc. Chem. Res.* **2001**, *34*, 80.

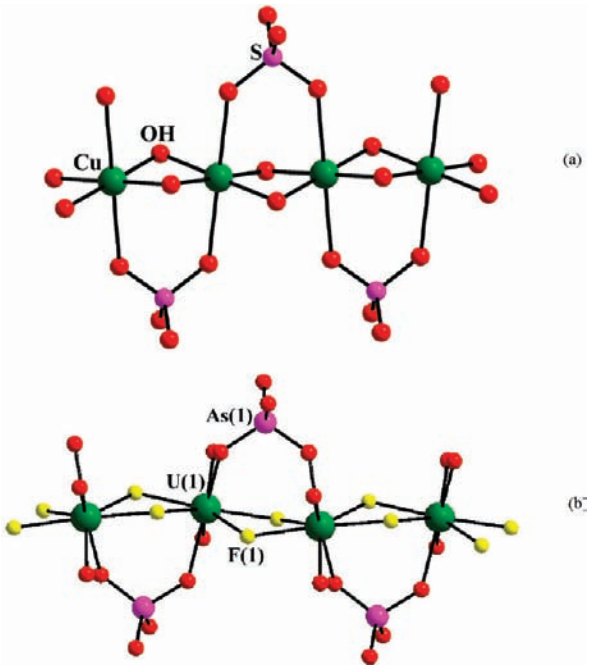

Figure 9. (a) View of the one-dimensional chains observed in the copper sulfate mineral *linarite*, $PbCu(SO_4)(OH)_2$.[25a,d] (b) View of the one-dimensional chain observed in $[C_2N_2H_9][UF_2(AsO_4)]$, **IV**.

retaining the same oxidation state of +6 as that of the starting source, $UO_2(OAc)_2 \cdot 2H_2O$.

The coordination environment around the uranium atom also exhibits changes from 6 (**I**) to 9 (**IV**). A close examination of the synthetic conditions indicates that the uranium species exhibits lower coordination in highly acidic pH and higher coordination at near neutral conditions. The variable nature of the uranium coordination chemistry has been reasonably realized in the present studies by variation of the pH of the reaction medium.

Mineralogical Relevance of the Structures. It has been known that many synthesized uranium containing compounds serve as model compounds for the minerals and have relevance to mineralogy.[25] The uranium arsenate structures, established during the present investigations, exhibit some similarities to the naturally occurring minerals. Thus, the layer arrangement observed in **I** resembles the layers in the mineral *autunite*, $Ca[(UO_2)(PO_4)]_2(H_2O)_{11}$.[25d,e] The layers in both the structures are formed by the vertex sharing between the uranium octahedra and the phosphate tetrahedra (Figure S10, Supporting Information). The interlayer spaces in *autunite* are occupied by Ca^{2+} ions, and in the present structure, $[C_2N_2H_9][(UO_2)(AsO_4)]$, **I**, protonated *en* molecules are present. The *autunite* layers have also been observed previously in arsenates.[6a]

The layer arrangement observed in $[C_2N_2H_{10}][(UO_2)F(HAsO_4)]_2 \cdot 4H_2O$, **II**, has close similarity to the aluminophosphate mineral *metavauxite*, $[Fe(H_2O)_6][Al(OH)(H_2O)(PO_4)]_2$.[25b,d] The layers in *metavauxite* are formed by the aluminum octahedra sharing the −OH vertices, and in **II**, the trans fluorine vertices connect the uranium centers. The Al−OH−Al chains are connected by the phosphate units forming the layer. The view of the layers in *metavauxite* and the uranium arsenate, $[C_2N_2H_{10}][(UO_2)F(HAsO_4)] \cdot 4H_2O$, **II**, is shown in Figure 8. The

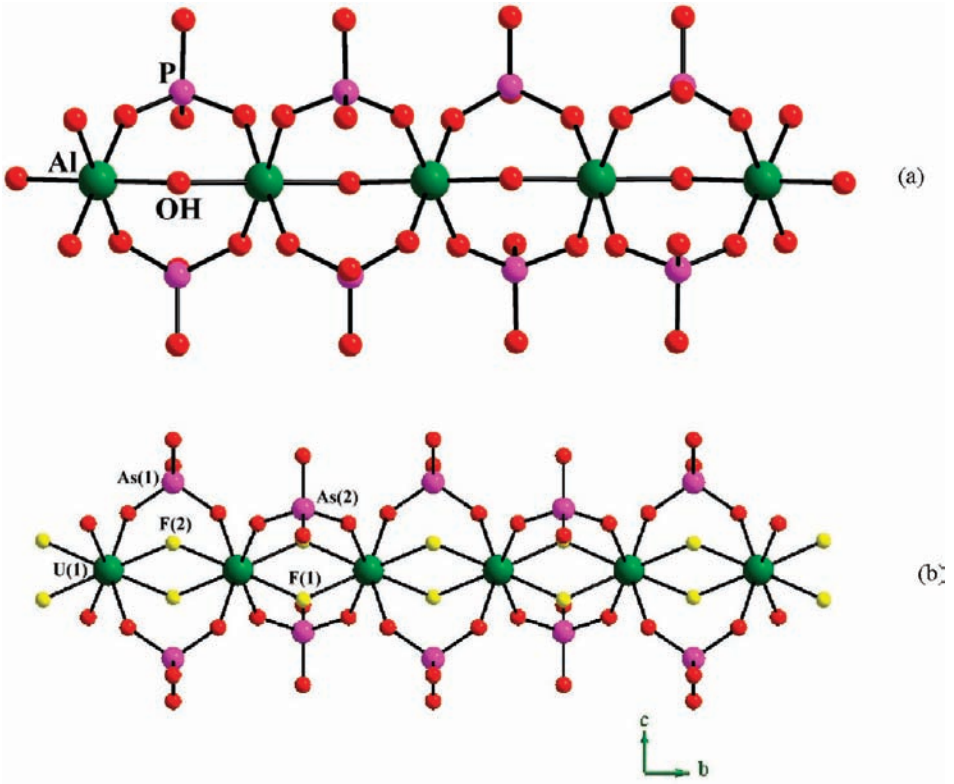

Figure 10. (a) View of the one-dimensional chain observed in the mineral *tancoite*, $LiNa_2H[Al(PO_4)_2(OH)]$.[25c,d] (b) View of the one-dimensional structure in $[C_4N_3H_{16}][U_2F_6(AsO_4)(HAsO_4)]$, **VI**.

layers are separated by $[Fe(H_2O)_6]^{2+}$ ions in *metavauxite*, whereas the protonated *en* molecules occupy the interlamellar spaces in **II** (Figure S11, Supporting Information and Figure 2b). *Metavauxite* related structures have been observed before in many uranium containing structures such as the uranium phosphate, $[(CH_3)_2NH(CH_2)_2NH(CH_3)_2][(UO_2)_2F_2(HPO4)_2]$,[7e] uranium sulfate, $[C_3N_2H_{12}][UO_2F(SO_4)]_2 \cdot H_2O$,[9d] and also in uranium selenate, $[NH_4][UO_2F(SeO_4)] \cdot H_2O$.[10a]

The one-dimensional uranium fluoroarsenate fragments observed in the structures of $[C_2N_2H_9][U_2F_5(HAsO_4)_2]$, **III**; $[C_2N_2H_9][UF_2(AsO_4)]$, **IV**; $[C_4N_3H_{16}][U_2F_3(AsO_4)_2(HAsO_4)]$, **V**; and $[C_4N_3H_{16}][U_2F_6(AsO_4)(HAsO_4)]$, **VI**, also have been observed in minerals. Thus, the one-dimensional uranium fluoroarsenate fragment $[UF_2(AsO_4)]_\infty$, in **IV**, is closely related to the mineral *linarite*, $PbCu(SO_4)(OH)_2$.[25a,d] In the *linarite* structure, the octahedral copper centers are connected through the −OH groups forming one-dimensional Cu−$(OH)_2$−Cu chains, on to which the sulfate groups anchor (Figure 9). In $[C_2N_2H_9][UF_2(AsO_4)]$, **IV**, we observe a similar arrangement involving the uranium and the arsenate units, except that the uranium centers are connected through the fluorine atoms (Figure 9). While the one-dimensional chains in **IV** are further connected to each other through the arsenate units forming the higher dimensional structure, the *linarite* mineral has a simple one-dimensional structure where the lead atoms bind to the three oxygens of the copper chain forming a trigonal pyramical coordination (Figure S12, Supporting Information). In the structure of **VI**, we observe a fragment of the structure that resembles the alumino-phosphate mineral *tancoite*, $LiNa_2H[Al(PO_4)_2(OH)]$.[25c,d] In *tancoite*, the octahedral aluminum centers are connected either by F^- or OH^- forming Al−F−(OH)−Al chains, on to which the phosphate units are bonded completing the one-dimensional chain structures. In the uranium arsenate structure **VI**, we find similar connectivity between the uranium centers except that the uranium centers are connected by two fluorine atoms forming U−F_2−U units, on to which the arsenate units are bonded (Figure 10). But the tancoite related structure is connected further forming a higher dimensional structure in the present compound.

In addition to the observation of the mineralogical structures, we have also found the well established building unit, SBU-4,[3b] in the structures of $[C_2N_2H_9][U_2F_5(HAsO_4)_2]$, **III**; $[C_4N_3H_{16}][U_2F_3(AsO_4)_2(HAsO_4)]$, **V**; and $[C_4N_3H_{16}][U_2F_6(AsO_4)(HAsO_4)]$, **VI**. SBU-4 units are connected through the edges forming one-dimensional chains in **III**, and in **VI** the SBU-4 units are connected throug their corners. Edge-shared SBU-4 units have been observed previously in an iron arsenate structure, $[C_4N_3H_{15}][Fe_2F_4(HAsO_4)_2]$.[4d] In **V**, the individual SBU-4 units are connected through additional oxygen giving rise to a new type of chain. In addition, this connectivity can also be considered to resemble the double crankshaft chains, especially when considering the basic connectivity between uranium and arsenic units (Figure 11). The double crankshaft chains are well established in many aluminosilicate and aluminophosphate structures.[27] A comparison of the two structures clearly reveals the close resemblance between the present

(27) Baerlocher, Ch.; McCusker, L. B.; Olson, D. H. *Atlas of Zeolite Framework Types*; Elsevier: Zurich, Switzerland, 2007.

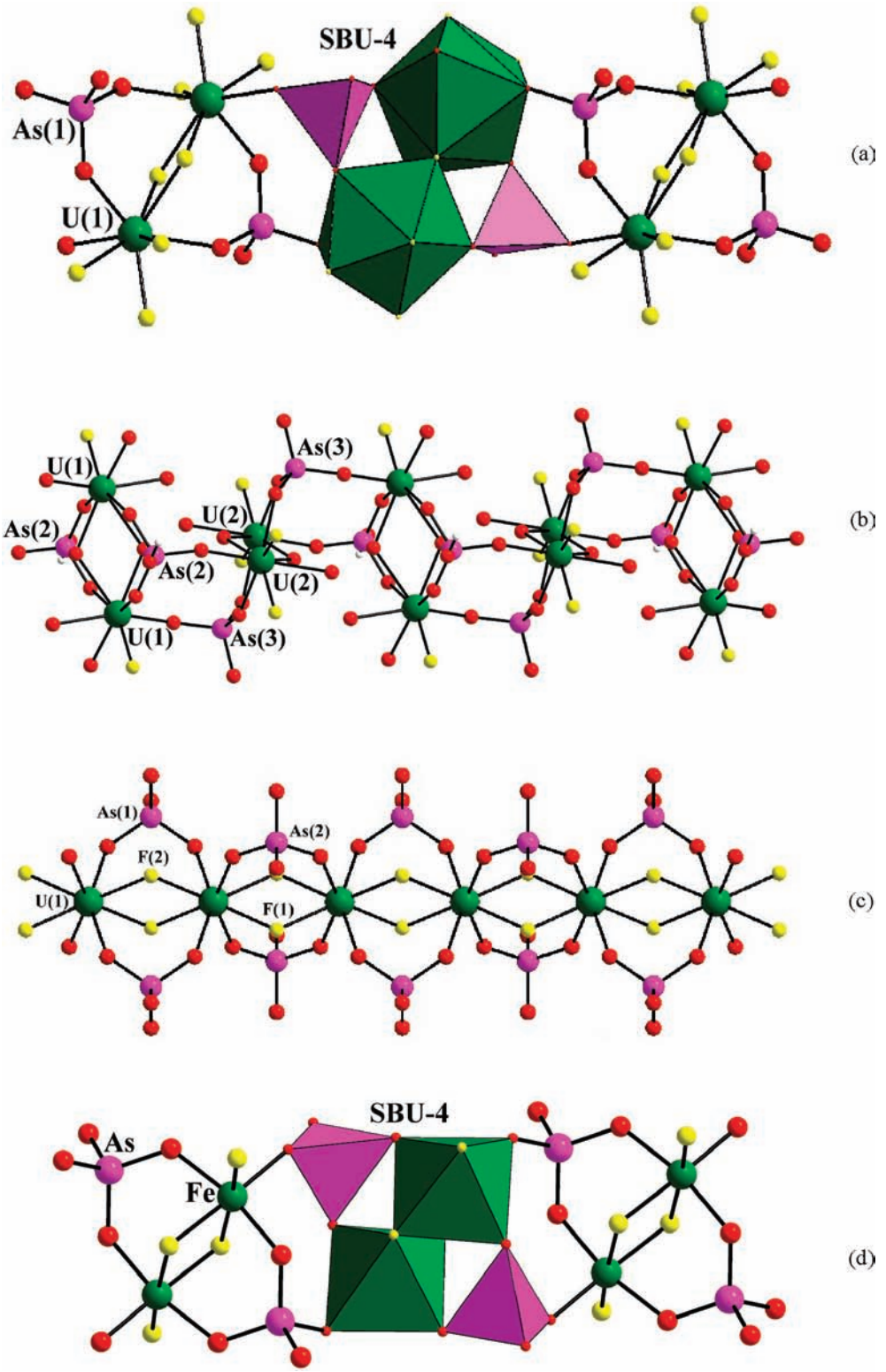

Figure 11. View of the one-dimensional chains formed from the SBU-4 units. (a) $[C_2N_2H_9][U_2F_5(HAsO_4)_2]$, **III**. (b) $[C_4N_3H_{16}][U_2F_3(AsO_4)_2(HAsO_4)]$, **V**. (c) $[C_4N_3H_{16}][U_2F_6(AsO_4)(HAsO_4)]$, **VI**. (d) $[C_4N_3H_{15}][Fe_2F_4(HAsO_4)_2]$.[4d] Note that all the chains are formed by the linkages involving the SBU-4 units (see text).

structure and the aluminophosphate structure (Figure S13, Supporting Information).

(28) (a) Auzel, F. *Proc. IEEE* **1973**, *61*, 758. (b) Blasse, G.; Grabmaier, B. C. *Luminescent Materials*; Springer: Berlin, 1994. (c) Auzel, F. *Chem. Rev.* **2004**, *104*, 139.

Optical Studies. It is known that the tetravalent uranium centers can exhibit characteristic absorption bands in the UV−vis region.[8b,28] The compound $[C_4N_3H_{16}][U_2F_6(AsO_4)(HAsO_4)]$, **VI**, has uranium in a +4 oxidation state and has been prepared as a pure phase which prompted us to examine the UV−vis spectroscopic

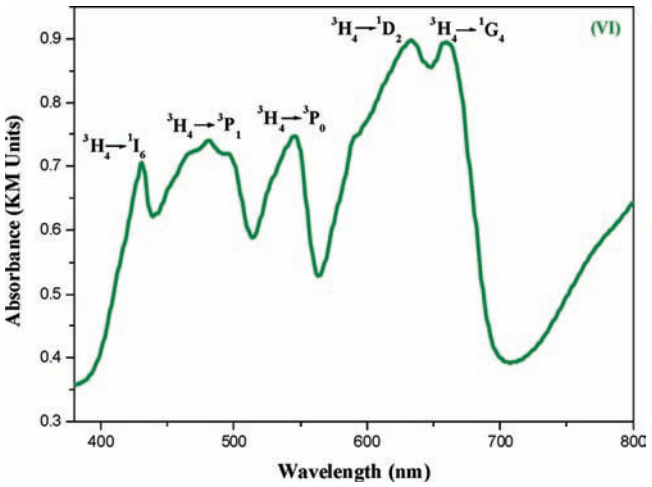

Figure 12. Room-temperature UV−vis spectrum of $[C_4N_3H_{16}][U_2F_6(AsO_4)(HAsO_4)]$, **VI**.

properties (Figure 12). The spectra showed characteristic bands, which could be identified, and some of the important absorption bands have been assigned: $^3H_4 \rightarrow {}^1G_4$ (658 nm), $^3H_4 \rightarrow {}^1D_2$ (634 nm), $^3H_4 \rightarrow {}^3P_0$ (545 nm), $^3H_4 \rightarrow {}^3P_1$ (498 nm), and $^3H_4 \rightarrow {}^1I_6$ (429 nm). The $^3H_4 \rightarrow {}^1I_6$ absorption band can be examined using an excitation wavelength of 498 nm. The photoluminescence spectrum of **VI** exhibited a strong emission band at 367 nm ($^1I_6 \rightarrow {}^3H_4$) along with two weak bands at 402 and 423 nm ($^3P_2 \rightarrow {}^3H_4$) (Figure 13a). The observation of a strong emission band at 367 nm, when excited using 498 nm wavelength light suggests that the compound absorbs more than one photon, probably involving an up-conversion process.[28] The up-conversion process could involve many different mechanisms, and in the present case, it is likely that the excitation may involve a two-stage pathway (A → B → C). If the difference in the energy levels of C and B and the levels of B and A are equal, and if the lifetime of B is not too short, the excitation radiation can excite the photon from A to B and then to C. The final emission can occur from C to A, and the emission could then be an *antistokes* emission. This process would facilitate detection of the infrared radiation visually. The up-conversion phenomenon of this type has been well established in lanthanide compounds, especially those involving Nd^{3+} ions.[29] A recent report on uranium(IV) phosphite also exhibited the up-conversion behavior.[8b] Since the compound $[C_4N_3H_{16}][U_2F_6(AsO_4)(HAsO_4)]$, **VI**, has uranium in a +4 oxidation state, we examined the emission behavior of **VI** carefully.

To understand and correlate the number of photons involved during the excitation process using 498 nm wavelength light, we have carried out power dependence studies (Table S2, Supporting Information). Similar power dependence studies have been employed before to understand the excitation and emission processes that involve more than one photon, and this has been described previously.[8b] During the present study, we used the same protocal and followed the emission intensities as

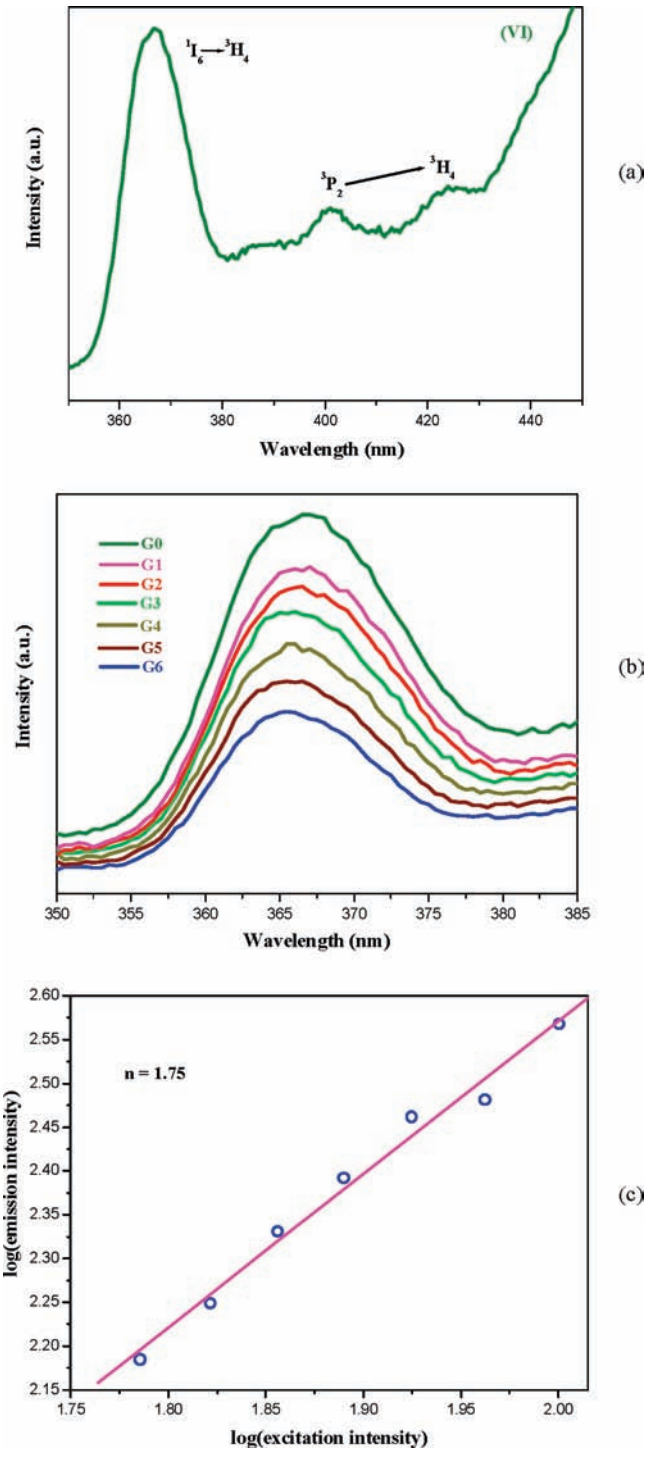

Figure 13. (a) Room temperature photoluminescence spectra of **VI** (λ_{ex} = 498 nm). Note that the main emission peak is observed at lower wavelengths (λ_{em} = 367 nm). (b) Observed emission dependence on the excitation intensity of the $^1I_6 \rightarrow {}^3H_4$ transition. (c) The log−log plot of the excitation intensity dependence of the luminescence intensity for λ = 498 nm.

a function of excitation intensity (Figure 13b). The log−log plot of the emission intensities of 367 nm ($^1I_6 \rightarrow {}^3H_4$) as a function of the incident intensity is shown in Figure 13c. A linear fit gave a value of 1.75 for *n*. This suggests that the photophysical behavior could involve two photons. A schematic of the possible energy-transfer processes for the U^{4+} ion is shown in Figure 14. As can be noted, the ground state ($^3H_4$) of the U^{4+} ion absorbs a

(29) Mahata, P.; Ramya, K. V.; Natarajan, S. *Chem.—Eur. J.* **2008**, *14*, 5839.

photon (498 nm) to reach an excited state $^3P_1$ (denoted by (1)) which nonradiatively could decay to the state $^3F_2$. The energy gap between the $^3F_2$ (first excited state) and the $^3H_4$ (ground state) level is reasonably large, prohibiting the complete nonradiative decay to the ground state. This would suggest that the $^3F_2$ level would have a reasonable lifetime and can be excited by the second photon to the $^3P_2$ and $^1I_6$ levels. The observed emissions from the U^{4+} ion result from the $^1I_6 \rightarrow {}^3H_4$ (367 nm) and $^3P_2 \rightarrow {}^3H_4$ (402 and 423 nm) transitions.

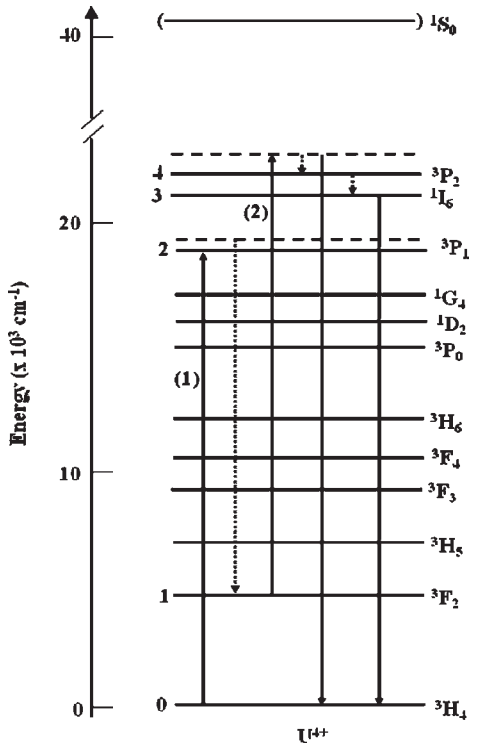

Figure 14. Schematic energy-level diagram for the various possible absorption and emission pathways for uranium in the +4 oxidation state. Dotted arrows represent the possible nonradiative decay processes. The upconversion behavior in **VI** is due to the two-photon absorption, ground state, and excited state absorptions (one photon, $^3H_4 \rightarrow {}^3P_1$; second photon, $^3F_2 \rightarrow {}^3P_2$, $^3F_2 \rightarrow {}^1I_6$; see text).

Magnetic Studies. Since the uranium atoms are in a +4 oxidation state in $[C_4N_3H_{16}][U_2F_6(AsO_4)(HAsO_4)]$, **VI**, we wanted to study the magnetic response as a function of the temperature of the compound. In addition, the presence of one-dimensional U−F−U chains indicates a possibility of stronger interactions between the U^{4+} centers (two unpaired electrons ($5f^2$)). The magnetic susceptibility measurements have been carried out on a powdered sample in the temperature range 3−300 K using a SQUID magnetometer (Quantum Design). The variable temperature magnetic response under zero-field cooled (ZFC) and field cooled (FC) conditions are shown in Figure 15. Both the ZFC and FC susceptibility data exhibit comparable behavior in the temperature range investigated in the present study. The high temperature data (50−300 K) were fitted to a Curie−Weiss behavior. A value of $C = 1.24$ cm^3 K mol^{-1} and $\theta p = -97.18$ K were obtained by this fit (Figure S16, Supporting Information). The observed effective magnetic moment per uranium atom was found to be 2.75 μ_B at 300 K, which is in good agreement with the presence of two unpaired electrons (2.7−3.6 μ_B). The negative θp value suggests antiferromagnetic behavior in **VI**. Similar values for the magnetic moments have been observed before for compounds containing uranium in the +4 oxidation state, e.g., $[C_2N_2H_{10}][U_2F_6(HPO_3)_2]$ ($\mu_{eff} = 2.75\ \mu_B$),[8b] $[C_4N_2H_{12}][U_2F_6(HPO_3)_2]$ ($\mu_{eff} = 2.85\ \mu_B$),[8b] $[C_5N_2H_{14}]_2[U_2F_{12}]\cdot H_2O$ (UFO-6, $\mu_{eff} = 3.53\ \mu_B$),[13e] $[C_5N_2H_{14}](H_3O)[U_2F_{11}]$ (UFO-7, $\mu_{eff} = 3.32\ \mu_B$),[13e] $[C_4N_2H_{12}]_2[U_2F_{12}]\cdot H_2O$ (UFO-9, $\mu_{eff} = 3.21\ \mu_B$),[13e] and $[C_6N_2H_{14}]_2[U_3O_4F_{12}]$ (UFO-17, $\mu_{eff} = 3.26\ \mu_B$)[13e]

Conclusions

Open-framework uranium arsenates with two- and three-dimensional structures have been synthesized and characterized. The uranium exhibits both the variable coordination and oxidation states in the compounds, which appears to have some correlation with the synthesis composition. The

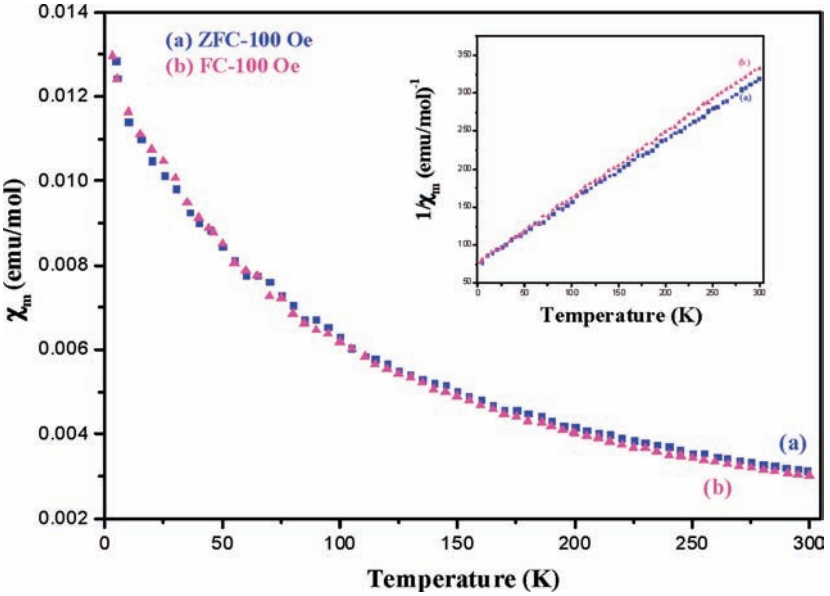

Figure 15. Variation of the magnetic susceptibility as a function of temperature for $[C_4N_3H_{16}][U_2F_6(AsO_4)(HAsO_4)]$, **VI**. Inset shows the $1/\chi_m$ vs T plot.

structures have close resemblance to some of the naturally occurring minerals, suggesting that the hydrothermal condition could replicate the geothermal conditions. The single-crystal-to-single-crystal transformation studies during the dehydration−hydration of the uranium arsenate, $[C_2N_2H_{10}][(UO_2)F(HAsO_4)]_2 \cdot 4H_2O$, **II**, give the first such observation in the family of uranium arsenates. The observation of a two-photon process during the photoluminescence study of $[C_4N_3H_{16}][U_2F_6(AsO_4)(HAsO_4)]$, **VI**, is noteworthy. Magnetic studies suggest antiferromagnetic interactions. The diversity of the structures, observed in the present study, suggests that the family of uranium arsenates can also exhibit considerable variations in the coordination around uranium as well as the structures. It is likely that many related phases can be prepared by careful choice of the reaction conditions. Work toward this goal is presently in progress.

Acknowledgment. The authors thank Professor P. K. Das of Inorganic and Physical Chemistry Department, Indian Institute of Science, Bangalore, India, for useful discussions on up-conversion studies. The authors also thank Professor K. V. Ramanujachary of Department of Chemistry and Biochemistry, Rowan University, New Jersey, for the magnetic measurements. S.N. thanks the Department of Science and Technology (DST), Government of India, for the award of a research grant and also for RAMANNA Fellowship. V.K.R. and M.C. thank the Council of Scientific and Industrial Research, Government of India, for the award of a research fellowship.

Supporting Information Available: Selected bond angles for **I**−**VI**, **IIa**, and **IIb** (Table S1); powder X-ray patterns of (a) simulated and (b) experimental results of **II** and **VI** (Figures S1 and S2); IR spectra of **II** and **VI** (Figure S3); TGA of **II** and **VI** (Figure S4); coordination geometry around the uranium ions and a possible model for the disorder of the amine molecules in **I** (Figure S5); coordination geometry around the uranium ions and hydrogen bond interactions between the water molecules in **II** (Figure S6); coordination geometry around the uranium ions, a possible model for the disorder of the amine molecules, and T-atom connectivities of three-dimensional structure along the [011] direction in **IV** (Figure S7); coordination geometry around the uranium ions, edge-connectivity of the arsenic with the uranium atoms, and double crank shaft chains observed in **V** (Figure S8); coordination geometry around the uranium ions, SBU-4 units, the T-atom connectivity, and a possible model for the disorder of the amine molecules in **VI** (Figure S9); arrangement of the layers in *autunite* mineral (Figure S10); arrangement of the layers in *metavauxite* mineral (Figure S11); connectivity of the chains in *linarite* mineral and in **IV** (Figure 12); T-atom connectivities of **V** and GIS (Figure S13); schematic representation of the structures, **III**, **V**, and **VI**, formed from SBU-4 units (Figure 14); plot of reversible water uptake study of **II** (Figure S15); plot of the effective magnetic moment vs T (Figure 16); data of power dependence studies on **VI** (Table S2). This material is available free of charge via the Internet at http://pubs.acs.org.